

## Stochastic dynamic instability response of piezoelectric functionally graded beams supported by elastic foundation

Niranjan L. Shegokar<sup>a</sup> and Achchhe Lal<sup>\*</sup>

*Department of Mechanical Engineering, S.V.N.I.T. Surat-395007, India*

*(Received November 5, 2015, Revised April 19, 2016, Accepted June 19, 2016)*

**Abstract.** This paper presents the dynamic instability analysis of un-damped elastically supported piezoelectric functionally graded (FG) beams subjected to in-plane static and dynamic periodic thermo-mechanical loadings with uncertain system properties. The elastic foundation model is assumed as one parameter Pasternak foundation with Winkler cubic nonlinearity. The piezoelectric FG beam is subjected to non-uniform temperature distribution with temperature dependent material properties. The Young's modulus and Poisson's ratio of ceramic, metal and piezoelectric, density of respective ceramic and metal, volume fraction exponent and foundation parameters are taken as uncertain system properties. The basic nonlinear formulation of the beam is based on higher order shear deformation theory (HSDT) with von-Karman strain kinematics. The governing deterministic static and dynamic random instability equation and regions is solved by Bolotin's approach with Newmark's time integration method combined with first order perturbation technique (FOPT). Typical numerical results in terms of the mean and standard deviation of dynamic instability analysis are presented to examine the effect of slenderness ratios, volume fraction exponents, foundation parameters, amplitude ratios, temperature increments and position of piezoelectric layers by changing the random system properties. The correctness of the present stochastic model is examined by comparing the results with direct Monte Carlo simulation (MCS).

**Keywords:** dynamic instability; functionally graded beams; Bolotin's approach; standard deviation; first order perturbation method; random system properties; elastic foundation; Monte Carlo simulation

### 1. Introduction

FG Materials are the advanced inhomogeneous composite materials, composed of two or more constitutes phases of metal and ceramic spatially varied in controlled directions by the variation of the volume fraction exponent of constituent materials. The metal constituent portion provides the mechanical strength, and toughness while, ceramics constituent provides high temperature withstanding ability and corrosion resistance. The appropriate mixing of metal and ceramic constituents open new possibilities for researchers to examine the performance and stabilities of thermal barrier of turbine blades, heat exchanger tubes, thermoelectric generators, furnace linings, cutting tools, metal ceramic joints etc.

A variety of light-weight heavy load bearing structural components such as aircraft wings,

---

<sup>\*</sup>Corresponding author, Assistant Professor, E-mail: [achchhelal@med.svnit.ac.in](mailto:achchhelal@med.svnit.ac.in), [lalachchhe@yahoo.co.in](mailto:lalachchhe@yahoo.co.in)

<sup>a</sup>Ph.D. Student, E-mail: [nir\\_shegokar@rediffmail.com](mailto:nir_shegokar@rediffmail.com)

helicopter rotors, turbine blades, spacecraft antennae, flexible satellites, robot arms, and long-span bridges can be modeled as FGM beam members. These structural components are sometimes may be subjected to different periodic in-plane and/or out-of-plane loadings and become dynamically unstable and produce parametric resonance conditions. For optimum high performance and safe design of such components, there is need of proper understanding of their instability behaviors and regions in stochastic sense.

For health monitoring purpose, attachment of surface bonded piezoelectric layers at the top and bottom of FG structures are needed, to make the structures, smart by self monitoring and self controlling performance capabilities under the action of external stimuli. Hence, effect of piezoelectric layers on the structural performance are extremely needed.

The FG beams supported by elastic foundations have been passed some important messages to the engineering community for stability and flexibility purposes. Such structures are being used as shocks observers and may be modeled as a flexible beam in ships and bridges, automobiles, spacecraft arms, footings, foundation of spillway dams, deep wells and civil buildings in cold regions. From practical point of views, Pasternak elastic foundation with Winkler cubic nonlinearity is proved as a more appropriate model for design prospective due to controlling of displacements along both of the longitudinal and transverse directions.

The volume fraction exponents, material properties of FG structures and surface bonded piezoelectric layers, density of constituent materials, and foundation parameters can be modeled as statistical random system variables. It is because of complete control of these random system variables at each design level is very difficult and challenging. The presence of these random system properties, may have significantly affected the structural performance particularly, dynamic instability. Hence, the effect of dispersion of these random system properties from their mean values in terms of standard deviation (SD) using stochastic approaches is needed for safe and reliable design.

Comprehensive study of deterministic dynamic stability problems for elastic structures of different shapes of beams, plates and shells is reported by many researchers. Notably among them are Abbas and Thomas (1978), Ahuja and Duffield (1975), Bolotin (1964), Evan-Iwanowski (1965), Bert and Birman (1987), Chen and Yang (1990), Ganpati *et al.* (1994), Ganpati *et al.* (1999), Datta *et al.* (1982), Patel *et al.* (2006), Wang and Dawe (2002), Moorthy *et al.* (1990), Srinivasan and Chellapandi (1986), Chattopadhyay and Radu (2000), Baldinger *et al.* (2000), Hu and Tzeng (2000), Singha *et al.* (2001), Young and Chen (1994), Liao and Cheng (1994), Sahu and Datta (2007), Wu *et al.* (2007), Yang *et al.* (2004), Pradyumna and Bandyopadhyaya (2010), Ng *et al.* (2001), Zhu *et al.* (2005), Darabi *et al.* (2007), Ke and Wang (2011), Mohantya and Dash (2011), Fu *et al.* (2012).

The fields related to stochastic analyses for the dynamic stability analysis of FG structures are very limited. Few efforts have been made in the past by the researchers, to quantify the different level of random system properties and their effects of structural performance using various probabilistic approaches.

In this direction, there are different probabilistic approaches are used for quantifying the several aspects of uncertainties at different variability levels in the materials, geometrical and/or external excitations as random processes (Kleiber and Hien 1992, Nigam and Narayana 1994, Iwankiewicz and Nielsen 1999, Nayfeh 1993, Namachchivaya *et al.* 2003). Shinozuka and Astill (1972) evaluated the expected mean value and variance of the vibration and buckling eigenvalues of a beam-column with random geometric and material properties using computerized Monte Carlo simulation and investigated the accuracy of perturbation method. Vanmarcke and Grigoriu (1983)

evaluated the second order statistics of deflection response of beam with random material properties through correlation method using direct MCS. Chang and Chang (1994) investigated the statistical dynamic responses of a non-uniform beam by using the stochastic finite element method in conjunction with perturbation technique and MCS with random change in Young's modulus of elasticity. Liu *et al.* (1986) presented the direct Monte Carlo simulation, stochastic finite element method and Hermite-Gauss quadrature probabilistic approaches to evaluate the statistics of dynamic response of truss and beam problem. Dey (1979) presented the applications of the stochastic finite element method, to analyze the response of multi-degree linear elastic structures subjected to stationary random stochastic loadings using matrix inversion and normal mode method. Ibrahim (1987) presented a review paper pertaining to structural dynamics with parameter uncertainties for two bar truss problems and highlighted the importance of perturbation, variational, asymptotic, and integral equation methods. Kareem and Sun (1990) investigated the influence of various level of damping uncertainties in the system dynamic response using second order perturbation technique (SOPT). Kapania and Perk (1996) evaluated the second-order sensitivity of the transient response and sensitivity with respect to various system parameters to single- and two-degree-of-freedom structural linear and nonlinear dynamic systems using central difference numerical approach. Zhao and Chen (1998) developed the new dynamic stochastic finite element method (FEM) by assuming uncertain dynamic shape function matrix based on dynamic constraint mode to study the dynamic response of spatial frame structures. Giuseppe (2011) presented a fully constraint theoretical framework of finite element (FE) based analysis with precise, intervalued and fuzzy probabilistic methods of linear mechanical systems. Rollet and Elishakoff (2003) used the conventional FEM combined with perturbation techniques in stochastic sense for getting a structural bending response of the beam with stochastic stiffness subjected to either deterministic or random loading. Ren *et al.* (1997) proposed a new version of FEM in conjunction with perturbation technique and MCS for mean and covariance function of displacements for bending beam using newly established variational approach. Stefanou *et al.* (2009) provided a state-of-art reviewed the applications and developments of stochastic finite element methods (SFEM) from past, recent and future aspects of the engineering applications. Yang *et al.* (2005) studied the thermo-mechanically induced bending responses of functionally graded plate with random system properties using Reddy's higher order shear deformation theory (HSDT) combined with FOPT. Raj *et al.* (1998) obtained the static response of graphite epoxy composite laminates with random material properties using HSDT combined with MCS. Onkar and Yadav (2005) evaluated the transverse central deflection response of laminated composite plate with random material properties and random external loading using Kirchoff-Love plate theory with von-Karman nonlinearity through FOPT. Lal *et al.* (2012a, 2012b, 2013) evaluated the second order statistics of initial and post buckling analysis of laminated composite and functionally graded plates subjected to thermo-mechanical loadings. They used HSDT based  $C^0$  nonlinear FEM combined with direct iterative based stochastic finite element methods using FOPT. Jagtap *et al.* (2011, 2013) evaluated the second order statistics of bending analysis of FGM plate using HSDT combined with direct iterative based nonlinear FEM in conjunction with FOPT. Shegokar and Lal (2013a, 2013b, 2014) evaluated the second order statistics of thermo-electro-mechanically induced bending, buckling and vibration response of the FGM beam with random system properties using HSDT combined with nonlinear FEM combined with FOPT and MCS. Lal *et al.* (2015) evaluated the finite element based thermo-mechanically induced post buckling response of elastically supported laminated composite plate with random system properties using HSDT with von-Karman nonlinear strain kinematics combined with second order perturbation

method (SOPT).

To the best of this author's knowledge, based on the HSDT, a stochastic thermo-mechanically induced nonlinear dynamic stability analysis of elastically supported FGM beams containing piezoelectric layers is not yet widely available in the literature. An intuitive prediction about instability behaviors and regions in terms of mean and SD of FGM beams subjected to in-plane non-conservative forces by accounting the random system properties at various variability levels are examined. In this study, a stochastic finite element formulation based on FOPT through HSDT with von-Karman nonlinearity is developed. In order to evaluate the dynamic instability regions, the Mathieu-Hill types equation using Bolotin's method is presented. The effect of slenderness ratios, volume fraction exponents, foundation parameters, amplitude ratios, temperature increments and position of piezoelectric layers by changing the uncorrelated random system properties on the mean and SD of dynamic instability analysis and regions of un-damped elastically supported FGM beam with surface bonded piezoelectric layers are examined.

## 2. Formulations

### 2.1 Geometric configurations and FGM properties

Let us consider a FGM rectangular beam with surface bonded piezoelectric layers supported by a Pasternak elastic foundation with Winkler cubic nonlinearity. The respective length and thickness of FGM beam are represented by  $L$  and  $h$  with the coordinate system  $(x, z)$  as shown in Fig. 1. At the top and bottom of the FGM beam, surface bonded piezoelectric layers of equal thickness ( $h_p$ ) are attached. The total thickness of FGM beam with piezoelectric layers is represented by  $H$ . It is assumed that a perfect bonding are existed among the FGM beam, surface bonded piezoelectric layers and supporting elastic foundations.

The foundation reaction per unit area ( $p$ ) exerted by supporting Pasternak elastic foundation with Winkler cubic nonlinearity can be represented as (Shegokar and Lal 2013a, 2013b)

$$p = K_1 w + K_3 w^3 - K_2 \partial^2 w / \partial x^2 \quad (1)$$

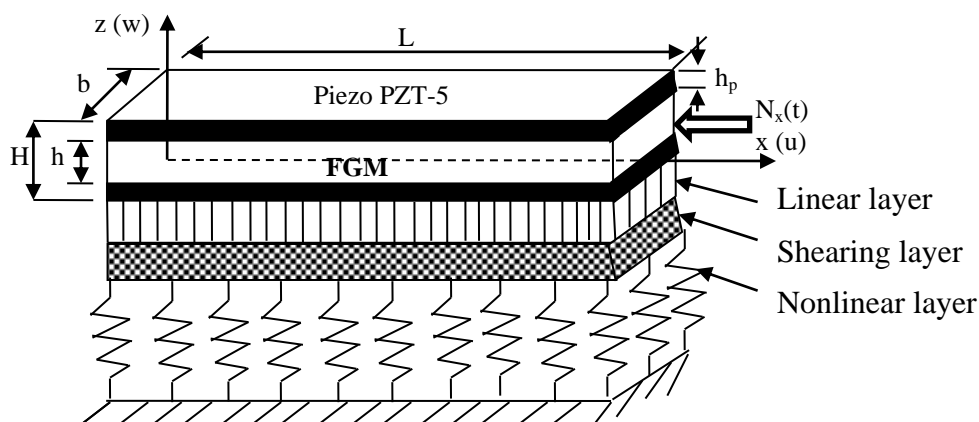


Fig. 1 Geometry of a piezoelectric FGM beam supported by elastic foundation

where  $w$ ,  $K_1$ ,  $K_3$  and  $K_2$  and are the transverse displacement of piezoelectric FGM beam, Winkler (spring) linear, nonlinear and Pasternak (shear) foundations, respectively.

It is assumed that FGM beam is composed from mixing of ceramic and metal constituents and the material compositions are varied continuously in the thickness direction, such a way that the top surface i.e.,  $z=h/2$  of the beam is ceramic rich, whereas the bottom surface i.e.,  $z=-h/2$  is metal rich.

The effective material properties  $P$ , can be expressed as

$$P = \sum_{k=1}^n P_k V_k \text{ with } \sum_{k=1}^n V_k = 1 \tag{2}$$

where  $P_k$  and  $V_k$  are the material properties and volume fraction of the constituent material  $k$ , that satisfying the volume fraction of all constituent materials.

For temperature dependent material properties, The effective material properties ( $P$ ) can be written as

$$P = P_0 \left( P_{-1}/T + 1 + P_1 T + P_2 T^2 + P_3 T^3 \right) \tag{3}$$

where  $P_i$  ( $i = -1, 0, 1, 2, 3$ ) are the coefficients of temperature  $T(K)$  and defined in Table 1.

For a FGM beam, the volume fraction of constituent material ( $k$ ) in the thickness direction ( $z$ ) can be written as

$$V_k(z) = \left( \frac{z}{h} + \frac{1}{2} \right)^n \tag{4}$$

where  $n$  is the volume fraction exponent and varies  $0 \leq n \leq \infty$  through the beam thickness.

The material properties of a FGM beam vary through thickness direction according to a power law distribution which is expressed as (Fu *et al.* 2012)

$$P(z) = (P_c - P_m)V_k(z) + P_m \tag{5}$$

where  $P_m$  and  $P_c$  represent the properties of metal and ceramic constituents, respectively.

### 2.2 Displacement field model

The modified displacement field components based on  $C^0$  continuity derived from Reddy's HSDT with seven degrees of freedom along coordinate directions can be written as (Shegokar and Lal (2013a, 2013b, 2014), Heyliger and Reddy (1988)

$$\bar{u}(x, z) = u_0(x) + z\psi_x - \frac{4}{3h^2} z^3 (\psi_x + \partial w / \partial x) \text{ and } \bar{w}(x, z) = w_0(x) \tag{6}$$

where  $u$  and  $w$  are the displacements along  $x$  and  $z$  directions, respectively. The parameters  $u_0$ ,  $w_0$  are the displacements of mid-plane, respectively. The symbols  $\psi_x$  and  $\theta_x$  are rotation and slope along  $x$ -direction, respectively.

The displacement vector consisting of four degree of freedoms (DOFs) can be written as

$$\{q\} = \{u \quad w \quad \theta_x \quad \psi_x\} \tag{7}$$

### 2.3 Stress- Strain relationship

The nonlinear thermo-piezoelectric material constitutive relationship between stress and strain for plane stress case, assuming large deformation theory with von-Karman nonlinearity can be written as

$$\bar{\sigma} = [Q](\bar{\varepsilon}) - [e]E_z \quad (8)$$

where  $[Q]$ ,  $\{\varepsilon\}$ ,  $[e]$  and  $\{E_z\}$  are the stiffness coefficient matrix, the strain vector, piezoelectric constant matrix and electric field vector for the one dimensional FGM beam, respectively and defined as

$$[Q] = \begin{bmatrix} Q_{11} & 0 \\ 0 & Q_{55} \end{bmatrix}, \{\varepsilon\} = \{\varepsilon_l\} + \{\varepsilon_{nl}\} - \{\varepsilon_t\} - \{E\}, [e] = \begin{bmatrix} 0 & e_{11} \\ e_{55} & 0 \end{bmatrix}, E_z = -\frac{\partial \phi_p}{\partial x} \quad (9)$$

here

$$Q_{11} = \frac{E(z)}{1-\nu^2}; Q_{55} = G(z) = \frac{E(z)}{2(1+\nu)} \quad (9a)$$

The linear strain vector  $\{\varepsilon_l\}$  using HSDT can be written as

$$\{\varepsilon_l\} = [T]\{\bar{\varepsilon}_l\} \quad (9b)$$

where  $[T]$  is the unit step vector with function of  $z$  and defined in Appendix A-1 and  $\{\bar{\varepsilon}_l\}$  is the reference plane linear strain tensor written as

$$\{\bar{\varepsilon}_l\} = \{\varepsilon_1^0 \quad k_1^0 \quad k_1^2 \quad \varepsilon_5^0 \quad k_5^2\} \quad (9c)$$

From Eq. (7), Eq. (9c) can be written as

$$\{\bar{\varepsilon}_l\} = [L]\{q\} \quad (9d)$$

where  $[L]$  is the differential operator defined in Appendix A-1.

The nonlinear strain vector  $\{\varepsilon_{nl}\}$  by assuming von-Karman strain kinematics is written as

$$\{\varepsilon_{nl}\} = \frac{1}{2}[A_{nl}]\{\phi_{nl}\} \quad (10)$$

$$[A_{nl}] = \frac{1}{2} \begin{bmatrix} \frac{\partial w}{\partial x} & 0 \\ 0 & 0 \end{bmatrix} \{\phi_{nl}\} = \begin{bmatrix} \frac{\partial w}{\partial x} \\ 0 \end{bmatrix} \quad (11)$$

The thermal strain vector  $\{\varepsilon_T\}$  and can be written as

$$\{\varepsilon_T\} = \{\alpha_x \Delta T \quad 0\} \quad (12)$$

where  $\alpha_x$  and  $\Delta T$  are the thermal expansion coefficient along  $x$  direction and nonuniform temperature change, respectively.

The non-uniform change in temperature ( $\Delta T$ ) along the thickness direction can be written as Kiani and Eslami (2010)

$$\Delta T = T(z) - T_0 \tag{13}$$

where,  $T_0$  is the reference temperature, i.e., room temperature and assumed to be 27°C.

The parameter  $T(z)$  is the steady state nonuniform temperature distribution and can be written as Shegokar and Lal (2013a)

$$T(z) = \begin{cases} T_p(z) & h/2 \leq z \leq h_p + h/2 \\ T_f(z) & h/2 \leq z \leq h/2 \\ T'_p(z) & -h_p - h/2 \leq z \leq h_p + h/2 \end{cases} \tag{14}$$

where  $T_p$ ,  $T'_p$  and  $T_f(z)$  are the temperature of the lower piezoelectric layer, upper piezoelectric layer and FGM layer, respectively.

The piezoelectric strain field vector  $E_z$  can be expressed as

$$\{E_z\} = [T_\phi] \{E^{(0)}\} \tag{15}$$

where  $T_\phi$  and  $E^0$  is the electric field potential operator and electric field vector respectively and defined as

$$[T_\phi] = \begin{bmatrix} 1 & z & z^2 & 0 & 0 \\ 0 & 0 & 0 & 1 & z \end{bmatrix} \{E^0\} = \begin{bmatrix} -\frac{\partial}{\partial x} & 0 & 0 \\ 0 & -\frac{\partial}{\partial x} & 0 \\ 0 & 0 & -\frac{\partial}{\partial x} \end{bmatrix} \begin{Bmatrix} \phi^{(0)} \\ \phi^{(1)} \\ \phi^{(2)} \end{Bmatrix} \tag{15a}$$

From Eq. (8), The parameters  $e_{11}$  and  $e_{13}$  are defined as Shegokar and Lal (2013b)

$$e_{11} = d_{11}Q_{11p} \text{ and } e_{13} = d_{15}Q_{55p} \tag{16}$$

where  $d_{11}$  and  $d_{15}$  are the dielectric constants. The parameters  $Q_{11p}$  and  $Q_{55p}$  are defined as

$$Q_{11p} = \frac{E_p}{1-\nu_p^2} \text{ and } Q_{55p} = \frac{E_p}{2(1+\nu_p)} \tag{16a}$$

From Eq. (8), the electric field vector  $E_z$  can be written as

$$E_z = -\frac{\partial \phi_p}{\partial x} \tag{16b}$$

where  $\phi_p$  is the electric field potential and can expressing as

$$\phi_p = N_\phi \varepsilon_z^\phi \tag{16c}$$

here,  $N_\phi$  and  $\varepsilon_z^\phi$  are the shape function matrix and electric potential DOFs vector and can be expressed as

$$\varepsilon_z^\phi = \{\phi_L \quad \phi_U\}^T \tag{16d}$$

The parameters  $\phi_L$  and  $\phi_U$  are electric potentials corresponding to lower and upper piezoelectric

layers, respectively.

## 2.4 Governing equation

The equation of motion can be derived using Hamilton's principle and expressed as

$$\delta\Pi = \int_{t_1}^{t_2} (\delta T - \delta U + \delta W) dt = 0 \quad (17)$$

where  $T$ ,  $U$  and  $W$  are the kinetic energy, the strain energy and the work done by the conservative buckling load of FGM beam with surface bonded piezoelectric layers supported by elastic foundation, respectively.

## 2.5 strain energy of the piezoelectric FGMs beam

The elastic strain energy of the piezoelectric FGM beam is written as Lal *et al.* (2015)

$$U = \frac{1}{2} \int_A \{\varepsilon\}^T \{\sigma\} dA - \frac{1}{2} \int_A \{E_z\}^T \{D_p\} dA, \quad (18)$$

where  $\{D_p\}$  is the electric field displacement vector and can be written as

$$\{D_p\} = [e]^T \{\varepsilon\} + [\xi] \{E_z\} \quad (19)$$

here  $[k]$  is the dielectric displacement coefficient matrix and defined as

$$[\xi] = \begin{bmatrix} \xi_{11} & 0 \\ 0 & \xi_{33} \end{bmatrix} \quad (19a)$$

Substituting Eq. (8), Eq. (19) in Eq. (17), once as obtains

$$U = \frac{1}{2} \int_A \left( \varepsilon^T [\bar{Q}\varepsilon - eE_z] - E_z^T [e^T \varepsilon + \xi E_z] \right) dA \quad (20)$$

Substituting Eqs. (9b), (9d) and Eq. (11) in Eq. (18), the linear potential energy ( $U_l$ ) of the piezoelectric FGMs beam can be further written as

$$U_l = \frac{1}{2} \int_A \left( q^T L^T D L q - q^T L^T D_1 L_\phi \phi_p - \phi_p^T L_\phi^T D_1^T L q - \phi_p^T L_\phi^T D_2 L_\phi \phi_p - q^T L^T F_l \right) dA \quad (21)$$

Where  $D$ ,  $D_1$  and  $D_2$ , are the elastic stiffness matrix of FGM and piezoelectric material, respectively, and defined in Appendix A-2 (a)-(c) substituting Eq. (9d) and Eq. (10c) in Eq. (17), the nonlinear potential energy ( $U_{nl}$ ) of piezoelectric beam can be further written as

$$U_{NL} = \frac{1}{2} \int_A \left( q^T L^T D_3 A_{nl} \phi_{nl} + A_{nl}^T \phi_{nl}^T D_4 q L + A_{nl}^T \phi_{nl}^T D_5 A_{nl} \phi_{nl} \varphi - A_{nl}^T \phi_{nl}^T D_6 L_\phi - L_\phi^T \phi_\varphi^T D_7 A_{nl} \phi_{nl} \right) dA \quad (22)$$

where  $D_3$ ,  $D_4$ ,  $D_5$ ,  $D_6$  and  $D_7$  are the elastic stiffness matrix of FGM and piezoelectric material, respectively and defined in Appendix A-3.

## 2.6 Strain energy due to elastic foundation

Using Eq. (1), the strain energy ( $U_f$ ) due to elastic foundation assuming Pasternak elastic foundation with Winklar cubic nonlinearity can be written as (Shegokar and Lal 2013a, 2013b)

$$\begin{aligned}
 U_f &= \frac{1}{2} \int_A \left[ K_1 (w)^2 + K_2 \left( \frac{\partial w}{\partial x} \right)^2 + K_3 (w)^4 \right] dA \\
 &= \frac{1}{2} \int_A \begin{Bmatrix} w \\ \frac{\partial w}{\partial x} \end{Bmatrix}^T \begin{bmatrix} K_1 & 0 \\ 0 & K_2 \end{bmatrix} \begin{Bmatrix} w \\ \frac{\partial w}{\partial x} \end{Bmatrix} dA + \frac{1}{2} \int_A \begin{Bmatrix} w \\ \frac{\partial w}{\partial x} \end{Bmatrix}^T \begin{bmatrix} K_3 w^2 & 0 \\ 0 & K_3 \end{bmatrix} \begin{Bmatrix} w \\ \frac{\partial w}{\partial x} \end{Bmatrix} dA
 \end{aligned}
 \tag{23}$$

Eq. (23) can be rewritten as

$$U_f = \frac{1}{2} \int_A \frac{1}{2} \boldsymbol{\varepsilon}_f^T \mathbf{D}_f \boldsymbol{\varepsilon}_f dA + \frac{1}{2} \int_A \frac{1}{2} \boldsymbol{\varepsilon}_f^T \mathbf{D}_{fnl} \boldsymbol{\varepsilon}_f dA
 \tag{23a}$$

where  $\boldsymbol{\varepsilon}_f = L_f w$  with  $L_f = \begin{bmatrix} 0 & 1 & 0 & 0 \\ 0 & \frac{\partial}{\partial x} & 0 & 0 \end{bmatrix}$   $\mathbf{D}_f = \begin{bmatrix} K_1 & 0 \\ 0 & K_2 \end{bmatrix}$   $\mathbf{D}_{fnl} = \begin{bmatrix} K_3 w^2 & 0 \\ 0 & 0 \end{bmatrix}$

### 2.7 Work done due to external in-plane mechanical loading

The potential due to external work done by the action of thermo-mechanical in-plane loading is written as

$$\delta W = -V = \frac{1}{2} \int_A \left[ N_x \left( \frac{\partial w}{\partial x} \right)^2 \right] dA
 \tag{24}$$

where,  $N_x$  is the in-plane thermo-mechanical loading known as axial compressive force and expressed in the following form

$$N_x = N_0 - N_0^T \text{ with } N_0^T = \int_{-h/2}^{h/2} (1, z, z^3) (Q_{11}) \alpha_x \Delta T dz
 \tag{25}$$

where  $N_x$  and  $N_t$  are the in-plane mechanical and thermal loads, respectively.

### 2.8 Kinetic energy of the FGM beam

The kinetic energy ( $T$ ) of the vibrating FGM beam can be expressed as

$$T = \frac{1}{2} \int_v \rho \{\dot{u}\}^T \{\dot{u}\} dv
 \tag{26}$$

where  $\rho$  and  $\{\dot{u}\}$  are the density and velocity vector of the FGM beam, respectively.

$$T = \frac{1}{2} \int_0^l \int_{-h/2}^{h/2} \rho(z) \left[ (\dot{u})^2 + (\dot{w})^2 \right] dz dx = \frac{1}{2} \int_0^l \int_{-h/2}^{h/2} \rho(z) [N]^T [N] dz dx
 \tag{26a}$$

### 3. Finite element formulation

The governing equation of the piezoelectric FGMs beam supported by elastic foundation, is derived using Hamilton principle given in Eq. (17). The FE analysis is performed using a 1-D Hermitian beam element with 4 DOFs per node.

Displacement vector  $\{q\}$  in Eq. (7) and Eq. (15d) can be written in terms of shape functions as

$$\{q\} = \sum_{i=1}^{NN} [N_i] \{q_i\} \quad \{\phi\} = \sum_{i=1}^{NN} [N_i] \{\phi_i\} \quad (27)$$

where  $i$  represent node number and  $N_i$  is shape function at  $i^{\text{th}}$  node.

For an element, the displacement field vector, and the electric potential vector can be written as

$$\{q\}^{(e)} = [N_i]^{(e)} \{q\}^{(e)} \quad \text{and} \quad \{\phi\}^{(e)} = [N]^{(e)} \{q_\phi\}^{(e)} \quad (27a)$$

Substituting Eq. (28) in Eq. (21), and summed over all elements using finite element model Eq. (27), Eq. (21) linear strain energy of the piezoelectric FGMs beam can be rewritten as

$$U_i^{(e)} = \sum_{i=1}^{NE} \left( q^{(e)T} K^{(e)} q^{(e)} - q^{(e)T} K1^{(e)} q_\phi^{(e)} - q_\phi^{(e)T} K1^{(e)T} q^{(e)} - q_\phi^{(e)T} K2^{(e)} q_\phi^{(e)} \right) \quad (28)$$

where

$$K^{(e)} = \frac{1}{2} \int_{A^{(e)}} B^{(e)T} D B^{(e)} dA, \quad K1^{(e)} = \frac{1}{2} \int_{A^{(e)}} B^{(e)T} D_1 B_\phi^{(e)} dA, \quad \text{and} \quad K2^{(e)} = \frac{1}{2} \int_{A^{(e)}} B_\phi^{(e)T} D_2 B_\phi^{(e)} dA, \quad (29)$$

Here  $K^{(e)}$ ,  $K1^{(e)}$  and  $K2^{(e)}$  are the element bending stiffness matrix, coupling matrix and dielectric matrix, respectively. The strain displacement matrix  $[B]$  for plate and piezoelectric  $[B_g]$  can be written as

$$[B]^{(e)} = [L][N_i]^{(e)}, \quad \text{and} \quad [B_\phi]^{(e)} = [L][N]^{(e)}. \quad (30)$$

with

$$[B]^{(e)} = [B_1 \quad B_2 \quad B_3 \quad \dots \quad B_{NN}] \quad \text{and} \quad [B_i] = [L]N_i, \quad \text{with} \quad i=1, 2, 3, \dots, NN \quad (30a)$$

the parameters  $L$  and  $N_i$  ( $i=1, \dots, 6$ ) are defined in Shegokar and Lal (2013a)

Similarly, using Eq. (28) in Eq. (22), and summed over all elements using finite element model Eq. (27), the nonlinear strain energy of the piezoelectric FGMs beam can be rewritten as

$$U_{nl}^{(e)} = \sum_{i=1}^{NE} \left( \{q^{(e)}\}^T k_1^{(e)} \{q^{(e)}\} + \{q^{(e)}\}^T k_2^{(e)} \{q^{(e)}\} + q^{(e)T} k_3^{(e)} \{q^{(e)}\} - \{q^{(e)}\}^T k_4^{(e)} \{q_\phi^{(e)}\} - \{q_\phi^{(e)}\}^T k_5^{(e)} \{q^{(e)}\} \right) \quad (31)$$

where the element bending stiffness matrix are

$$k_1^{(e)} = \frac{1}{2} \int_{A^e} B^{(e)T} D_3 \{A^{(e)}\} \{G^{(e)}\} dx dy \quad k_2^{(e)} = \frac{1}{2} \int_{A^e} \{G^{(e)}\}^T \{A^e\}^T D_4 \{B^{(e)}\} dx dy$$

$$k_3^{(e)} = \frac{1}{2} \int_{A^e} \{G^{(e)}\}^T \{A^{(e)}\}^T D_5 \{A^{(e)}\} \{G^{(e)}\} dx dy \quad (31a)$$

and the coupling matrix are

$$k_4^{(e)} = \frac{1}{2} \int_{A^e} \{G^{(e)}\}^T \{A^{(e)}\}^T D_6 \{B_\phi\} dx dy \quad k_5^{(e)} = \frac{1}{2} \int_{A^e} \{B_\phi^{(e)}\}^T D_7 \{A^{(e)}\} \{G^{(e)}\} dx dy \quad (31b)$$

Similarly, strain energy due to foundation after summing over all the elements using Eq. (27), Eq. (23) can be rewritten as

$$U_f^{(e)} = \sum_{i=1}^{NE} \{q^{(e)}\}^T K_{fl}^{(e)} \{q^{(e)}\} + \sum_{i=1}^{NE} \{q^{(e)}\}^T K_{fnl}^{(e)} \{q^{(e)}\} \quad (32)$$

where  $K_{fl}^{(e)} = \frac{1}{2} \int_{A^{(e)}} B_f^{(e)T} D_{fl} B_f^{(e)} dA$ , and  $K_{fnl}^{(e)} = \frac{1}{2} \int_{A^{(e)}} B_f^{(e)T} D_{fnl} B_f^{(e)} dA$  are the linear and nonlinear foundation stiffness matrix and  $[B_f]$  is the strain displacement matrix due to foundation and defined as

$$[B_f]^{(e)} = [L_f] [N_i]^{(e)} \quad (33)$$

Using a finite element model as Eq. (27), potential of work done due to thermo-mechanical loading as given Eq. (24) can also be written as

$$\delta W^{(e)} = \sum_{i=1}^{NE} \{q^{(e)}\}^T N_x K_g^{(e)} \{q^{(e)}\} \quad (34)$$

Where  $N_x$ ,  $[K_g]^{(e)}$  is defined as a thermal buckling load and elemental geometric stiffness matrix, respectively. The value of  $[K_g]$  is defined in  $K_g^{(e)} = \frac{1}{2} \int_{A^{(e)}} B_g^{(e)T} [N_o] B_g^{(e)} dA$

Using finite element analysis Eq. (27), after summing over all the elements, the kinetic energy of FGMs beam as given in Eq. (26a) can be written as (Shegokar and Lal 2013).

$$T = \sum_{e=1}^{NE} \left\{ \dot{q} \right\}^{(e)T} [M]^{(e)} \left\{ \dot{q} \right\}^{(e)} \quad (35)$$

where,  $[M]$  is the global consistent mass matrix.

Adopting numerical integration, the element bending stiffness matrix consist of linear and nonlinear, coupling matrix, dielectric stiffness matrix, foundation stiffness matrix, geometric stiffness matrix and mass matrix can be obtained by transforming expression in  $(x)$  coordinate system to natural coordinate system  $(\zeta)$  using Gauss quadrature method.

Substituting Eq. (28), Eq. (31), Eq. (32), Eq. (34) and Eq. (35) in Eq. (17), once obtains as (Lal et al. 2015)

$$\begin{bmatrix} M & 0 \\ 0 & 0 \end{bmatrix} \begin{Bmatrix} \ddot{q} \\ \ddot{\phi} \end{Bmatrix} + \begin{bmatrix} \lambda K_g & 0 \\ 0 & 0 \end{bmatrix} \begin{Bmatrix} q \\ \phi \end{Bmatrix} + \begin{bmatrix} K_{fl} & 0 \\ K_{fnl} & 0 \end{bmatrix} \begin{Bmatrix} q \\ \phi \end{Bmatrix} + \begin{bmatrix} K & K_1 \\ K_1^T & K_2 \end{bmatrix} \begin{Bmatrix} q \\ \phi \end{Bmatrix} = F_t \quad (36)$$

The Eq. (36) can be rewritten as

$$[M] \{\ddot{q}\} + [K - N_x K_g] \{q\} = [F_t] \quad (37)$$

where  $K = K_q + K_f + K_{fnl} - K_{q\_phi} K_{phi}^{-1} K_{q\_phi}^T$  with  $K_q = \sum_{e=1}^{NE} (K^{(e)} + K_1^{(e)} + K_2^{(e)})$

$$K_{q\_phi} = \sum_{e=1}^{NE} (K1^{(e)} + K_4^{(e)}); \quad K_{phi} = \sum_{e=1}^{NE} K2^{(e)}; \quad F_t = \sum_{e=1}^{NE} F_t^{(e)};$$

$$K_{fl} = \sum_{e=1}^{NE} K_{fl}^{(e)}; \quad K_{fnl} = \sum_{e=1}^{NE} K_{fnl}^{(e)}; \quad M = \sum_{e=1}^{NE} m^{(e)}$$

The parameters  $K_q, K_{q\_phi}, K_1^T, K_{phi}, F_t, K_{fl}, K_{fnl}$  and  $M$  are the global elastic stiffness matrix, coupling matrix between elastic mechanical and electrical effect, dielectric stiffness matrix, force vector and linear and nonlinear foundation stiffness matrix and mass matrix, respectively.

### 4. Instability analysis

The stability analysis of piezoelectric FG beam is performed by expressing the uniform pulsating axial compressive force  $N_x$ , in terms of a static and dynamic components, both are them written in terms of the critical buckling load,  $N_{cr}$ , and expressed as (Datta and Chakraborti 1982, Pryadumna and Bandyopadhyay 2010)

$$N_x = (N_s + N_t \cos \Omega t) = \alpha N_{cr} + \beta N_{cr} \cos \Omega t \tag{38}$$

where  $N_s$  and  $N_t$  are the static and dynamic portion of the in-plane load, respectively. The parameters  $\alpha, \beta$  and  $\Omega$  are the static load factor, dynamic load factors and frequency of excitation, respectively.

Substituting Eq. (38), in Eq. (37), the governing equation of beam in the form of instability equation can be further written as

$$[M]\{\ddot{q}\} + [K + \alpha N_{cr} K_g + \beta N_{cr} K_g \cos \Omega t]\{q\} = 0 \tag{39}$$

Eq. (39) is known as Mathieu-hill equation, describes the nonlinear instability behavior of the piezoelectric FGM beam of second order partial differential equation with periodic coefficients.

The boundaries between stable and unstable regions are formed by periodic solution of period  $T$  and  $2T$ , where  $T=2\pi/\omega$ . The boundaries of stable and unstable regions within period  $2T$  are of great practical importance and the solutions are performed in the form of trigonometric series as

$$q\{t\} = \sum_{k=1,3,5}^{\infty} \left[ \{a_k\} \sin \frac{k\omega t}{2} + \{b_k\} \cos \frac{k\omega t}{2} \right] \tag{40}$$

Substituting, Eq. (40) into Eq. (39) and considering only the first term of the series for the instability regions and then equating the coefficients of  $\sin(\omega t/2)\cos(\omega t/2)$ , Eq. (39) reduced to the form as

$$\left[ [K] - \left( \alpha \pm \frac{\beta}{2} \right) N_{cr} [K_g] - \left( \frac{\Omega}{\omega} \right)^2 \frac{\omega^2}{4} [M] \right] \{q\} = 0 \tag{41}$$

Eq. (41) represents an eigenvalue problem for the known value of  $\alpha, \beta$  and  $N_{cr}$ . The two conditions under the plus and minus signs corresponded to two boundaries (left and right) of the

instability regions are represented by  $\beta$ . The eigenvalues ( $\Omega/\omega$ ), give the boundary frequencies (known as disturbing frequency or resonance frequency) of the instability regions for the given values of  $\alpha$  and  $\beta$ . The problem is now reduced to that of finding the critical excitation frequency from the above equation. For a given value of  $\alpha$ , the variation of the eigenvalue ( $\Omega/\omega$ ) with respect to  $\beta$  can be found using standard eigenvalue algorithms. In Eq. (41), the value of  $N_{cr}$  is evaluated by assuming the static buckling critical load. The plot of such variations in the  $\beta$ - ( $\Omega/\omega$ ) plane shows the instability regions of the FGM beam subjected to the periodic axial load.

In the indirect approach, for the evaluation of transverse dynamic central deflection response internal in-plane force vector at the equilibrium condition for the given time  $t+\Delta t$  are needed. The in-plane internal force using Newton's second law of motion can be written as (Ganpathi *et al.* 1994, 1999)

$$[M]\{\ddot{q}\}_{t+\Delta t} + [[N(q)]\{q\}]_{t+\Delta t} = 0 \tag{42}$$

where  $\{\ddot{q}\}_{t+\Delta t}$  and  $\{q\}_{t+\Delta t}$  are the vectors of the nodal accelerations and displacement at time  $t+\Delta t$ , respectively. Substituting  $[M]\{\ddot{q}\}_{t+\Delta t}$  from Eq. (42) in Eq. (39), once obtains as

$$[[N(q)]\{q\}]_{t+\Delta t} = ([K] + N_{cr}(\alpha + \beta \cos \Omega t)[K_g])\{q\}_{t+\Delta t} \tag{43}$$

The, internal in-plane force vector  $[[N(q)]\{q\}]_{t+\Delta t}$  from Eq. (43) can be further written as

$$[[N(q)]\{q\}]_{t+\Delta t} = [[N(q)]\{q\}]_t + [K_T(q)]_t \{\Delta q\} \tag{44}$$

where,  $[[N(q)]\{q\}]_t$  is the internal in-plane force at time  $t$  and  $\{\Delta q\} = \{q\}_{t+\Delta t} - \{q\}_t$ . The parameter  $[K_T(q)]$  is the tangent stiffness matrix and defined as

$$[K_T(q)]_t = ([K] + N_{cr}(\alpha + \beta \cos \Omega t)[K_g])\{q\}_{t+\Delta t} \tag{45}$$

Substituting Eq. (45) into Eq. (42), one obtains the governing equation at  $t+\Delta t$  as

$$[M]\{\ddot{q}\}_{t+\Delta t} + [K_T(q)]_t \{\Delta q\} = -[[N(q)]\{q\}]_t \tag{46}$$

Eq. (46) is the nonlinear forced vibration equation and for the solution of this equation, the direct iterative procedure combined with the Newton-Raphson method with required convergence less than 1% tolerance is used.

For solution of Eq. (46) nonlinear Equilibrium is achieved for each time step through a modified Newton Raphson iteration scheme until the required convergence criteria is satisfied within the specific tolerance limit of less than 1%.

At time  $t+\Delta t$ , Eq. (46) can be further written as

$$[K^*]\{q\}_{t+\Delta t} = \{F\}_{t+\Delta t} \tag{47}$$

where  $[K^*]$  and  $\{F\}_t$  are the effective stiffness matrix and effective force vector, respectively defined as

$$[K^*] = \frac{1}{\beta \Delta t^2} [M] + [K_T(q)] \tag{48}$$

$$\{F\}_t = [M] \left( \frac{1}{\beta \Delta t^2} \{q\}_t + \frac{1}{\beta \Delta t^2} \{\dot{q}\}_t + \frac{1-2\beta}{2\beta} \{\ddot{q}\}_t \right) \quad (49)$$

here  $\{\dot{q}\}_{t+\Delta t}$  and  $\{\ddot{q}\}_{t+\Delta t}$  are the velocity and acceleration vectors at time  $t+\Delta t$ , respectively and are written as

$$\{\dot{q}\}_{t+\Delta t} = \{\dot{q}\}_t + \Delta t \left\{ (1-\gamma) \{\ddot{q}\}_t + \gamma \{\ddot{q}\}_{t+\Delta t} \right\} \quad (50)$$

$$\{\ddot{q}\}_{t+\Delta t} = \frac{1}{\beta \Delta t^2} \left[ \{q\}_{t+\Delta t} - \{q\}_t - (\Delta t) \{\dot{q}\}_t - (\Delta t)^2 \left( \frac{1}{2} - \beta \right) \{\ddot{q}\}_t \right] \quad (51)$$

The parameters  $\beta$  and  $\gamma$  are constants whose values depend on the finite difference used in the calculations. Here, the constant-average acceleration method is used which is implicit and unconditionally stable. Although the velocity vector is not required in standard dynamic Eq. (49), however, it is presented here because it will be needed subsequently. For this method the value of  $\beta$  and  $\gamma$  are taken as 1/4 and 1/2, respectively.

Eq. (51) is the dynamic stability deflection problem which is random in nature, being dependent on the system properties. Therefore, the eigenvalue and eigenvectors also become random. In deterministic environment, the solution of Eq. (51) is evaluated using standard time integration solution procedure such as central deflection, Wilson's, Newmark etc. However, in random environment, it is not possible to obtain the solution using the above mentioned numerical methods.

For this purpose, the direct iterative method is first time successfully combined with mean centered FOPT i.e., direct iterative based stochastic finite element method (DISFEM), developed by authors for dynamic instability analysis to obtain the second order statistic (mean and SD) of nonlinear dynamic transverse central deflection.

## 5. Solution approach

The nonlinear random forced vibration problem as given in Eq. (52) is solved by employing a direct iterative method in conjunction with the mean centered perturbation technique assuming that the random changes in transverse displacement during iterations and time does not affect the nonlinear stiffness matrix as the procedure given by Shegokar and Lal (2012), Jagtap *et al.* (2011). The systematic solution procedure for stochastic dynamic stability analysis using direct iterative based stochastic finite element method (DISFEM) is shown in Fig. 2.

### 5.1 Perturbation method

In the given Eq. (39), the operating random system variables can be expanded using Taylor series expansion about the mean values of random variables up to second order without loss of any generality as (Vanmarcke and Grigoriu 1983, Chang and Chang 1994)

$$\begin{aligned} [K^*] &= [K_0^*] + \sum_{i=1}^N [K_i^{*I}] \alpha_i; \quad \{q_i\} = \{q_{0i}\} + \sum_{i=1}^N \{q_i^{*I}\} \alpha_i; \\ [M] &= [M_0] + \sum_{i=1}^N [M_i^{*I}] \alpha_i; \quad \text{and } (\Omega/\omega)_i = (\Omega/\omega)_{0i} + \sum_{i=1}^N (\Omega/\omega)_i^I \alpha_i \end{aligned} \quad (52)$$

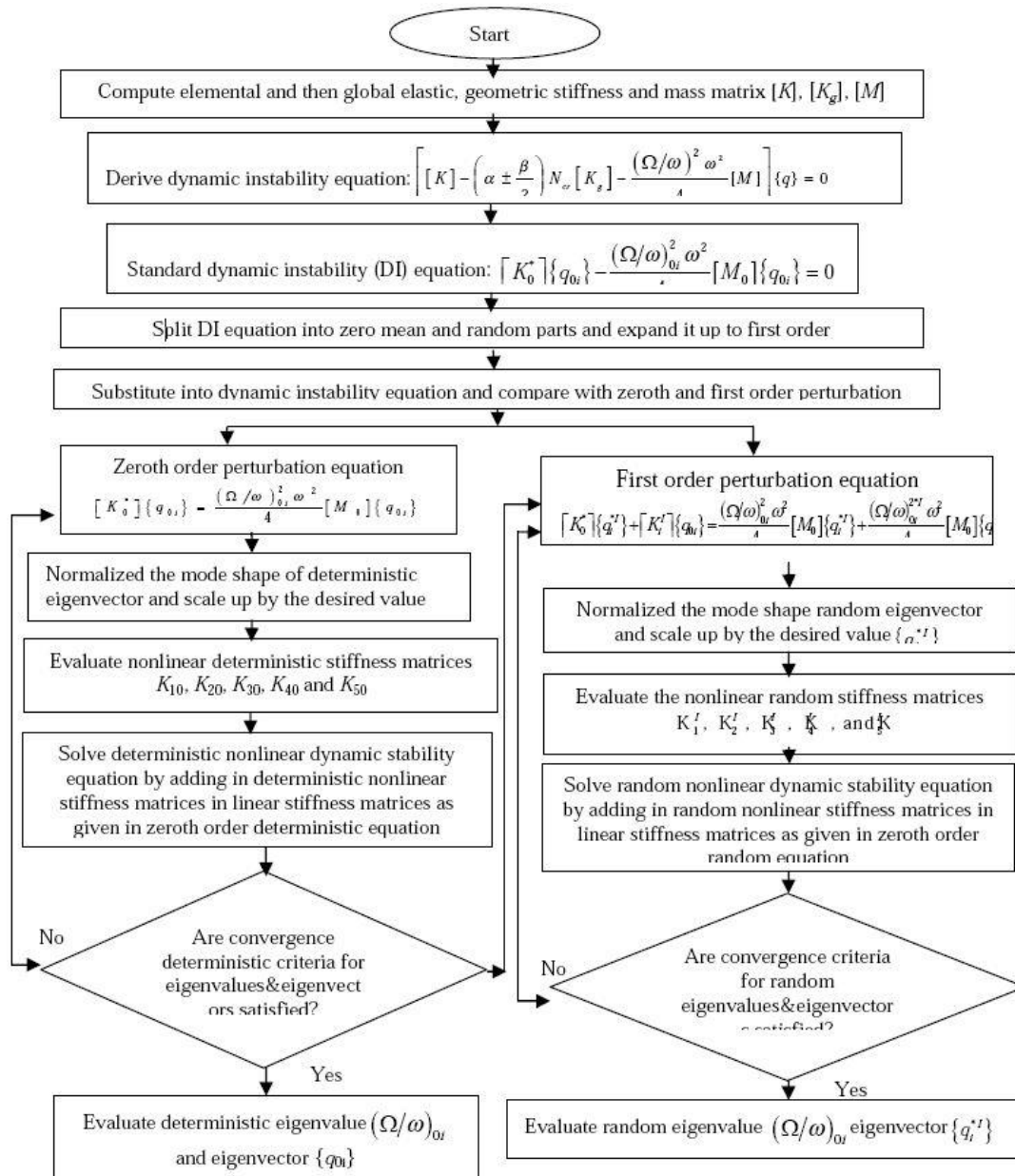


Fig. 2 Flow chart of solution procedure of stochastic dynamic stability analysis

where  $[K_0]$ ,  $[M_0]$ ,  $(\Omega/\omega)_0$  and  $\{q_0\}$  are the mean deterministic values of respective tensors. The parameters  $\alpha_i$  ( $i=1, \dots, b_n$ ) is statistically independent random variables ( $b_n$ ). The

symbol  $( )_i^{*r}$  represents the first order derivatives evaluated at  $\alpha=0$ , i.e.,  $K_i^{*r} = \left. \frac{\partial K}{\partial \alpha_i} \right|_{\alpha=0}$

Substituting Eq. (55) in Eq. (39) and after simplification following equations are obtained

$$[K_0^*]\{q_{0i}\} = \frac{(\Omega/\omega)_{0i}^2 \omega^2}{4} [M_0]\{q_{0i}\} \tag{53}$$

$$[K_0^*]\{q_i^{*I}\} + [K_i^{*I}]\{q_{0i}\} = \frac{(\Omega/\omega)_{0i}^2 \omega^2}{4} [M_0]\{q_i^{*I}\} + \frac{(\Omega/\omega)_i^{2*1} \omega^2}{4} [M_0]\{q_{0i}\} \tag{54}$$

The zeroth order Eq. (53) is a deterministic eigenvalue equation relating to mean quantities. The mean eigenvalues and corresponding eigenvectors can be evaluated using conventional eigensolution procedures. On the other side, first order Eq. (54) represents the random counterpart and the solution of random eigenvalues and corresponding eigenvectors can be evaluated using solution stochastic/probabilistic approach. In this approach, the eigenvector is normalized using orthogonality conditions to make it complete ortho-normal set. The orthogonality conditions for eigenvector can be written as (Shaker *et al.* 2008)

$$\begin{aligned} \{q_{0i}\}^T [M_0]\{q_{0j}\} &= \delta_{ij} \quad (i \neq j, \delta_{ij} = 0 \text{ and } i = j, \delta_{ij} = 1) \\ \{q_{0i}\}^T [K_0^*]\{q_{0i}\} &= \delta_{ij} \omega_{0i} \end{aligned} \tag{55}$$

The variance values for first order natural frequency are written as

$$Var[(\Omega/\omega), (\Omega/\omega)] \approx \sum_{i=1}^N \sum_{j=1}^N \{(\Omega/\omega)_i^{*I}\} \{(\Omega/\omega)_j^{*I}\}^T COV[\alpha_i, \alpha_j] \tag{56}$$

where  $N$  is the total number of random variables and The  $COV[\alpha_i, \alpha_j]$  is the covariance between  $\alpha_i$ , and  $\alpha_j$  can be evaluated in terms of correlation coefficients  $\rho_{ij}$  and expressed as (Shegokar and Lal 2013a, 2013b)

$$COV[\alpha_i, \alpha_j] = \sum_{i=1}^N \sum_{j=1}^N [C][C'] \tag{57}$$

where  $[C]$  and  $[C']$  can be written as

$$[C] = \begin{bmatrix} \sigma_{\alpha_1}^2 & cov(\alpha_1, \alpha_2) & \dots & cov(\alpha_1, \alpha_i) \\ cov(\alpha_2, \alpha_1) & \sigma_{\alpha_2}^2 & \dots & cov(\alpha_2, \alpha_i) \\ \dots & \dots & \dots & \dots \\ cov(\alpha_i, \alpha_1) & cov(\alpha_i, \alpha_2) & \dots & \sigma_{\alpha_i}^2 \end{bmatrix} \text{ and } [C'] = \begin{bmatrix} 1 & \rho_{\alpha_1, \alpha_2} & \dots & \rho_{\alpha_1, \alpha_i} \\ \rho_{\alpha_2, \alpha_1} & 1 & \dots & \rho_{\alpha_2, \alpha_i} \\ \dots & \dots & \dots & \dots \\ \rho_{\alpha_i, \alpha_1} & \rho_{\alpha_i, \alpha_2} & \dots & 1 \end{bmatrix}$$

where  $\sigma_{\alpha_i}$  is the standard deviation of random system variables and defined as

$$\sigma_{\alpha_i} = \mu_{\alpha_i} Var(\alpha_i) \tag{58}$$

where  $\mu_{\alpha_i}$  is the mean values of input random variables and  $Var(\alpha_i)$  is the variance of random variables from their mean values. Here,  $Cov[\alpha_i, \alpha_j]$  is a covariance matrix between two random variables and zero for independent random variables. The standard deviation (SD) can be evaluated by the square root of variance.

Using the procedure as mentioned above, from Eq. (47), the first order variance of deflection at time  $t+\Delta t$  can be written as (Shegokar and Lal 2013a, 2013b)

$$Var^I [q_{t+\Delta t}, q_{t+\Delta t}] \approx \sum_{i=1}^N \sum_{j=1}^N \{q_{i(t+\Delta t)}^{*I}\} \{q_{j(t+\Delta t)}^{*I}\}^T COV[\alpha_i, \alpha_j] \tag{59}$$



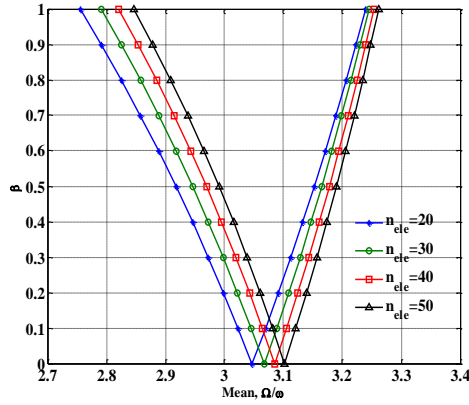


Fig. 3 Convergence study for the dynamic instability regions versus dynamic in-plane load parameters,  $\beta$

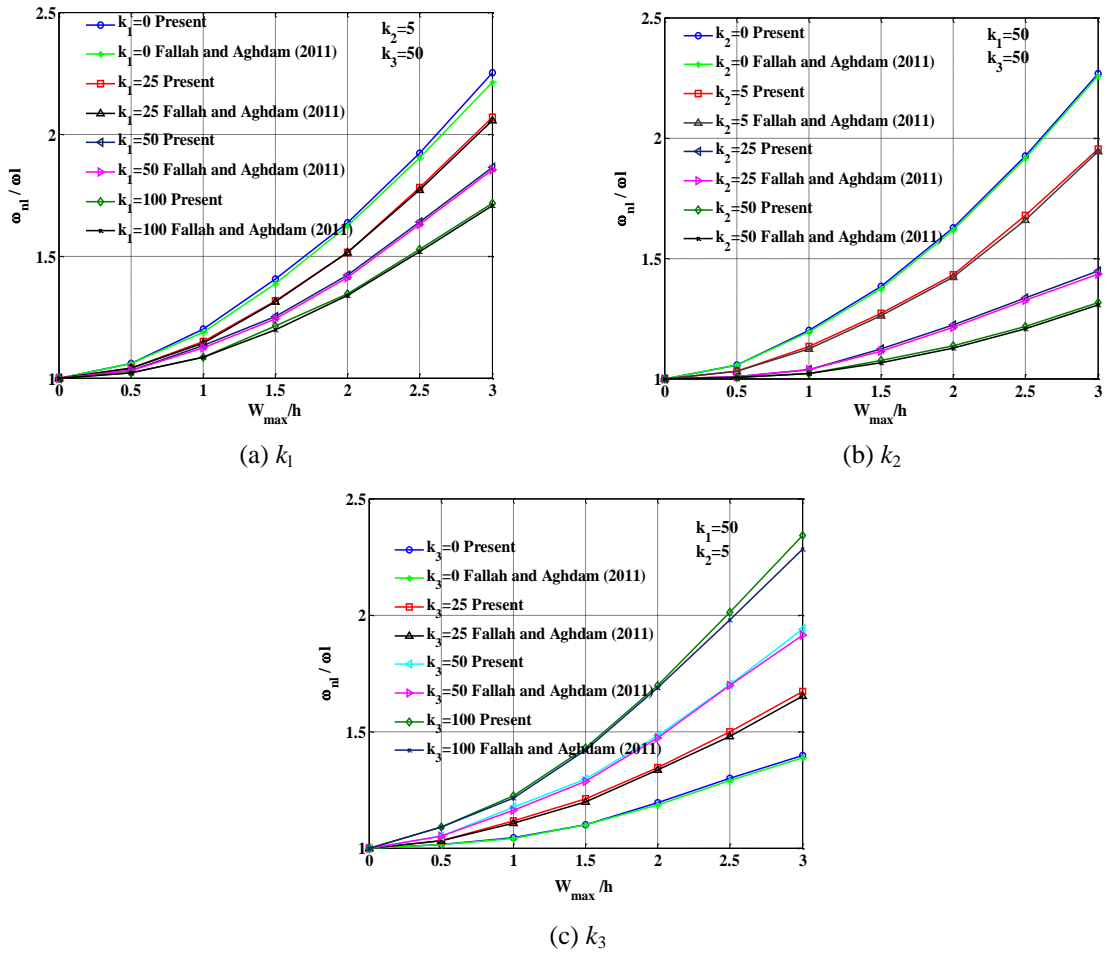


Fig. 4 Validation study for variation of amplitude ratios with foundation parameters  $k_1$ ,  $k_2$  and  $k_3$  on the frequency ratio of simply supported functionally graded beam

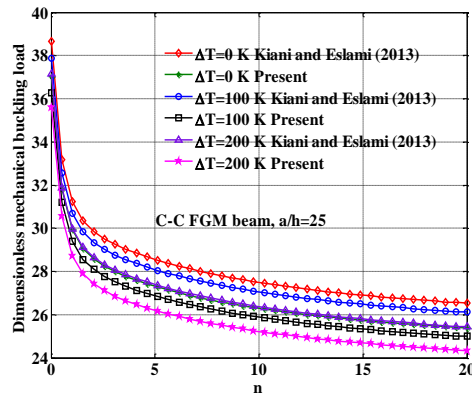


Fig. 5 Validation study for variation of volume fraction exponents with temperature change on the mechanical buckling of FGM beam

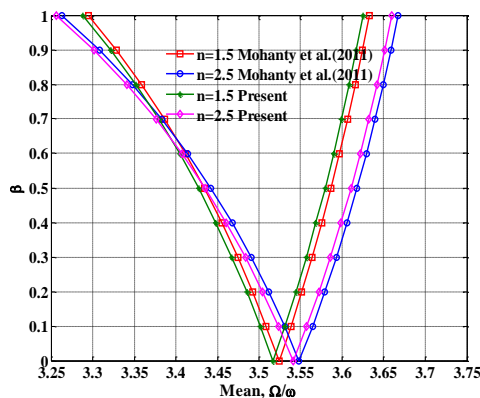


Fig. 6 Comparison of the primary instability regions versus dynamic in-plane load parameters,  $\beta$  for FGM beam

clear that as the number of elements increases, the dynamic instability regions are converged. Hence, for the further computation of results, total 30 elements are used.

The comparative study of the effects of different foundation parameters with amplitude ratios ( $W_{max}/h$ ) on the nonlinear fundamental frequency ratios ( $\omega_n/\omega_1$ ) of simply supported functionally graded beam are shown in Fig. 4(a)-(c) and compared with the published results of Fallah and Aghdam (2011). Present results using HSDT based finite element analysis (FEA) are in good agreements with published results of using an analytical approach. For the given amplitude ratio with the increase of foundation parameters, the frequency ratio decreases. Although with the increase of amplitude ratios, the frequency ratio increases. It is because of both the foundation parameters and amplitude ratio increase the stiffness of the beam. Among the different foundation parameters, the effect of the shear foundation parameter is highest as compared to other foundation foundations.

The effect of volume fraction exponents and temperature increments on mechanical buckling of FGM beam with a clamped-clamped support condition of temperature dependent material

properties and uniform temperature distribution is shown in Fig. 5 and compared with published results of Kiyani and Eslami (2013). For the different volume fraction exponents and temperature increments, the present results using HSDT with FEA are in good agreements with published results using first order shear deformation theory (FSDT) with an analytical approach.

6.2 Validation study for deterministic and probabilistic approach

Fig. 6 shows the comparison study of the dynamic instability by variations of volume fraction exponents for simply supported FGMs beam for  $a/h=25$  with Mohanty *et al.* (2011). With the increase in the volume fraction exponent, the dynamic instability occurs at a higher disturbing frequency and width of instability regions also increases. The present numerical results using HSDT with  $C^0$  FEM analysis for different volume fraction exponents are good agreement with the results of Mohanty *et al.* (2011) using FSDT with an analytical approach.

The comparison study in terms of the mean and standard deviation of dynamic stability of present FE based perturbation stochastic model is performed with the direct Monte Carlo simulation by variations of slenderness ratios ( $a/h$ ) for piezoelectric FGMs beam as shown in Fig. 7. With the increase of slenderness ratios, the mean and corresponding SD of dynamic instability occurs at a lower disturbing frequency. The width of instability regions for mean and correspond SD also increases with increase the slenderness ratios. However, by assuming random system parameters, the width of instability regions for SD by changing slenderness ratios are more severe. For the various values of slenderness ratios, the present FOPT based stochastic model is in good agreements with direct MCS. The detailed procedure for application of MCS on buckling and vibration problem is given in Ref. Shegokar and Lal (2013a, 2013b and 2014). It is noted that for Figs. 3 to 10 and 12 to 17, TD material properties with mechanical loading is considered while, for Fig. 13 thermomechanical load is considered. It is also noted that for the standard deviation of dynamic instability analysis, all random system properties are taken as uncorrelated and simultaneously varied as  $\{b_i (i=1, \dots, 10) = 0.10\}$  with  $\alpha=0.5$  and  $n=1$  (unless specified otherwise).

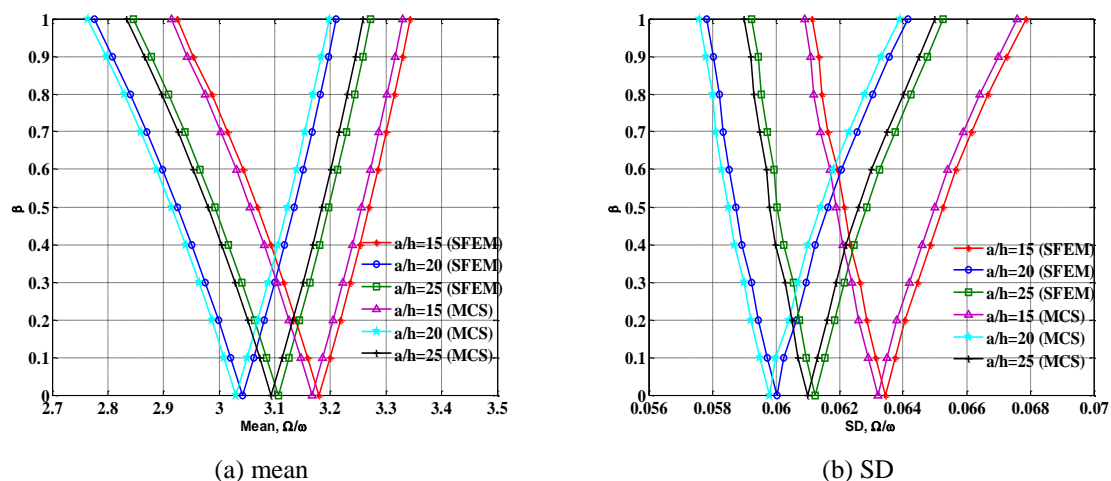


Fig. 7 Effect of the slenderness ratios on the dynamic instability region with random material properties  $\{b_i (i=1, \dots, 10) = 0.1\}$  of piezoelectric FGM beams

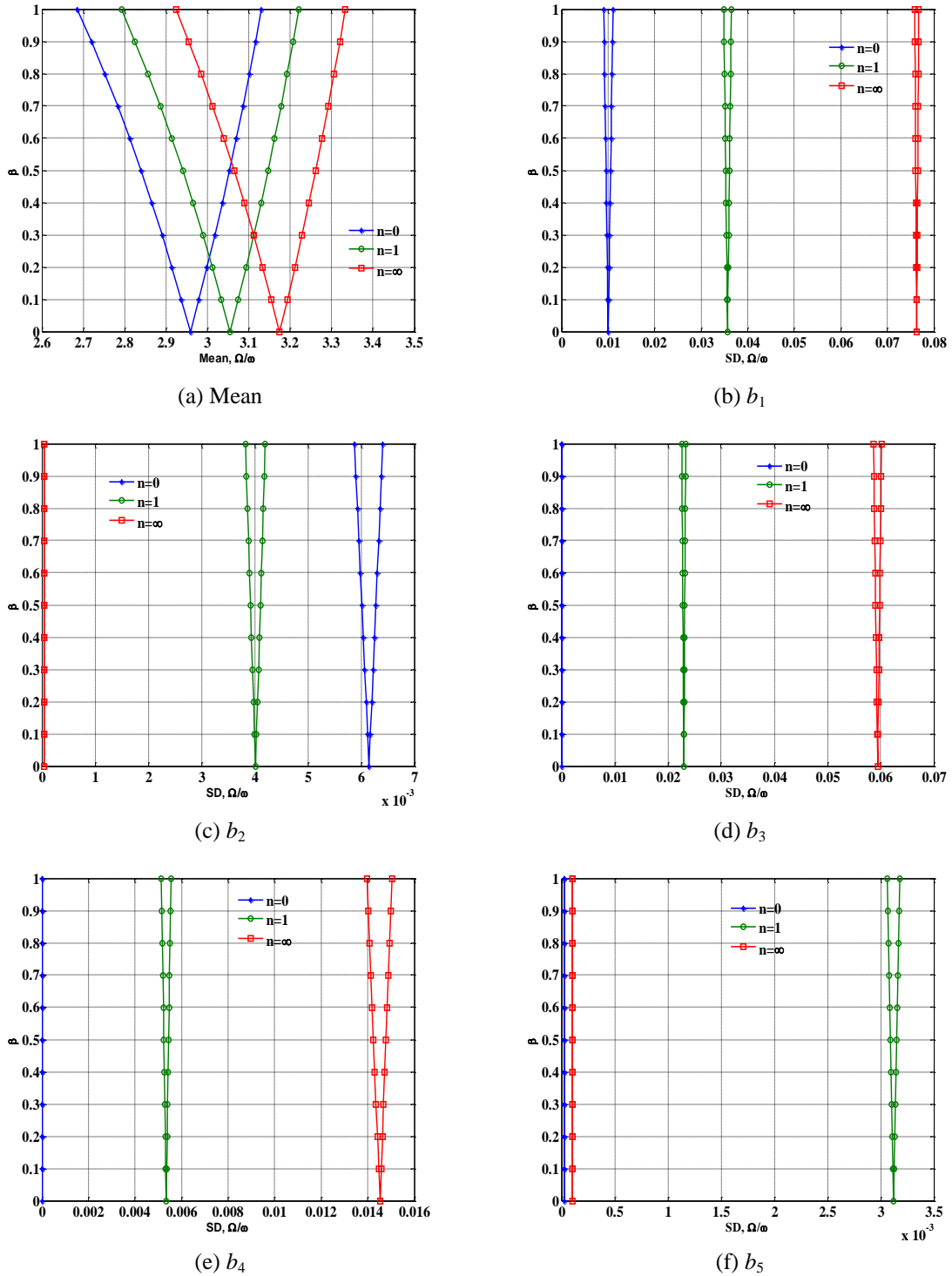


Fig. 8 Effect of individual random system properties with volume fraction exponents ( $n=0, 1.0,$  and  $\infty$ ) on the dynamic instability for (a) mean and corresponding SD with random change in  $b_1, b_2, b_3, b_4$  and  $b_5$

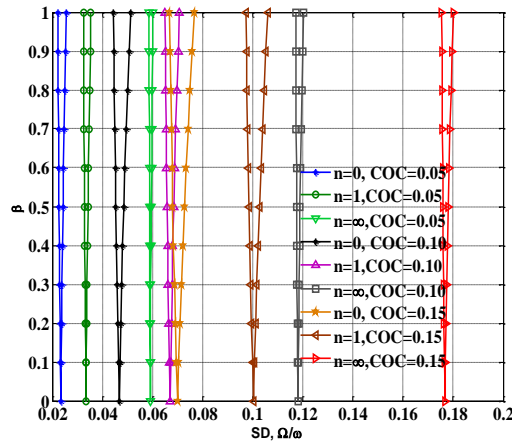


Fig. 9 Effect of coefficient of variation (COC) of random system properties up to 15% from their mean values with volume fraction exponents on the SD of dynamic instability of FGM beam

### 6.3 Parametric study for second order statistics of dynamic stability

The effect of volume fraction exponents ( $n=0, 1.0, \text{ and } \infty$ ) with random change in individual random system parameters  $\{b_i = (1, \dots, 5) = 0.15\}$  on the mean and SD of dynamic instability of simply supported FG plate for  $a/h=30$  is shown in Fig. 8 (a)-(f). The effect of individual change in respective densities of metal and ceramic, foundation parameters on the SD of dynamic instability and instability regions are highly effective. Hence, proper controls of these random system parameters are required for high reliability of the elastically supported piezoelectric FGM beam. With the increase of volume fraction exponents, the origin of stability region shifts to lower excitation frequency and instability regions becomes narrow.

The effect of a change in coefficient of variation (COC) of random system parameters  $\{b_i = (1, \dots, 10) = 0.05, \dots, 0.2\}$  on the SD of dynamic instability of simply supported FG plate for  $a/h=30$  is shown in Fig. 9. As the SD of random system properties and volume fraction exponents increase, the origin of SD of dynamic instability shifts to lower excitation frequency and width of dynamic instability increases and increment is more severe for higher SD of random change in system properties with whole FGM consists of ceramic portion.

Fig. 10 shows the effect of nonlinearity ( $W_{\max/h} = 0, 0.5, 1, 1.5$ ) on the mean and SD  $\{b_i (i=1, \dots, 10) = 0.1\}$  of the instability region of piezoelectric FGM beams for volume fraction exponents  $n=1.0$  and  $a/h=20$ . It is observed that the instability regions shift to higher disturbing frequency and the instability region becomes narrow as the linear model changes to the nonlinear model.

As the amplitude increases, the width of the instability region of FGM beam decreases and the origin of instability region shifts to higher excitation frequency. It is also observed that the origin of SD of dynamic instability shifts to higher excitation frequency and instability regions become narrow as the amplitude ratio increases.

The effect of different combinations of foundation parameters on the mean and SD  $\{b_i (i=1, \dots, 10) = 0.1\}$  of the dynamic instability region for  $n=1.0$  and  $a/h=20$  is shown in Fig. 11(a)-(d). With the increase of foundation parameters, the mean instability regions shift to higher excitation

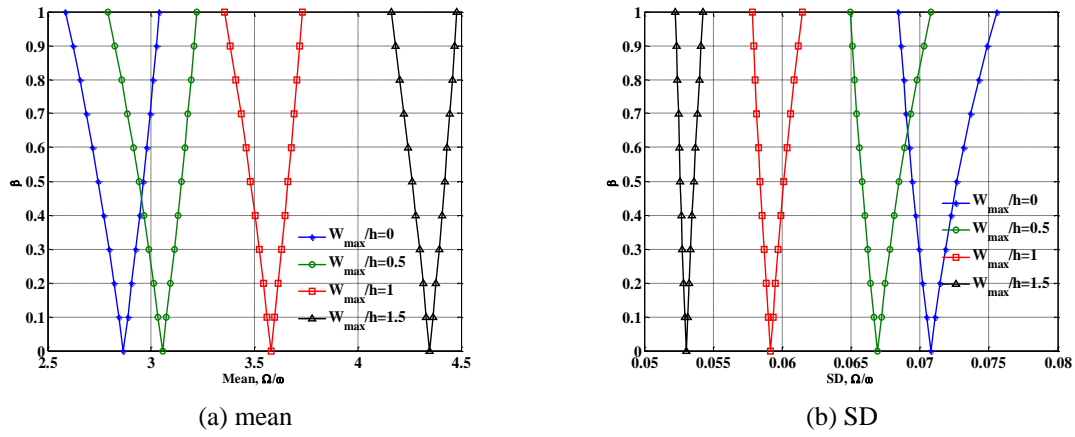


Fig. 10 Effect of theamplitude ratios ( $W_{max}/h=0, 0.5, 1, 1.5$ ) on the dynamic instability region of piezoelectric FGM beams with random material properties.

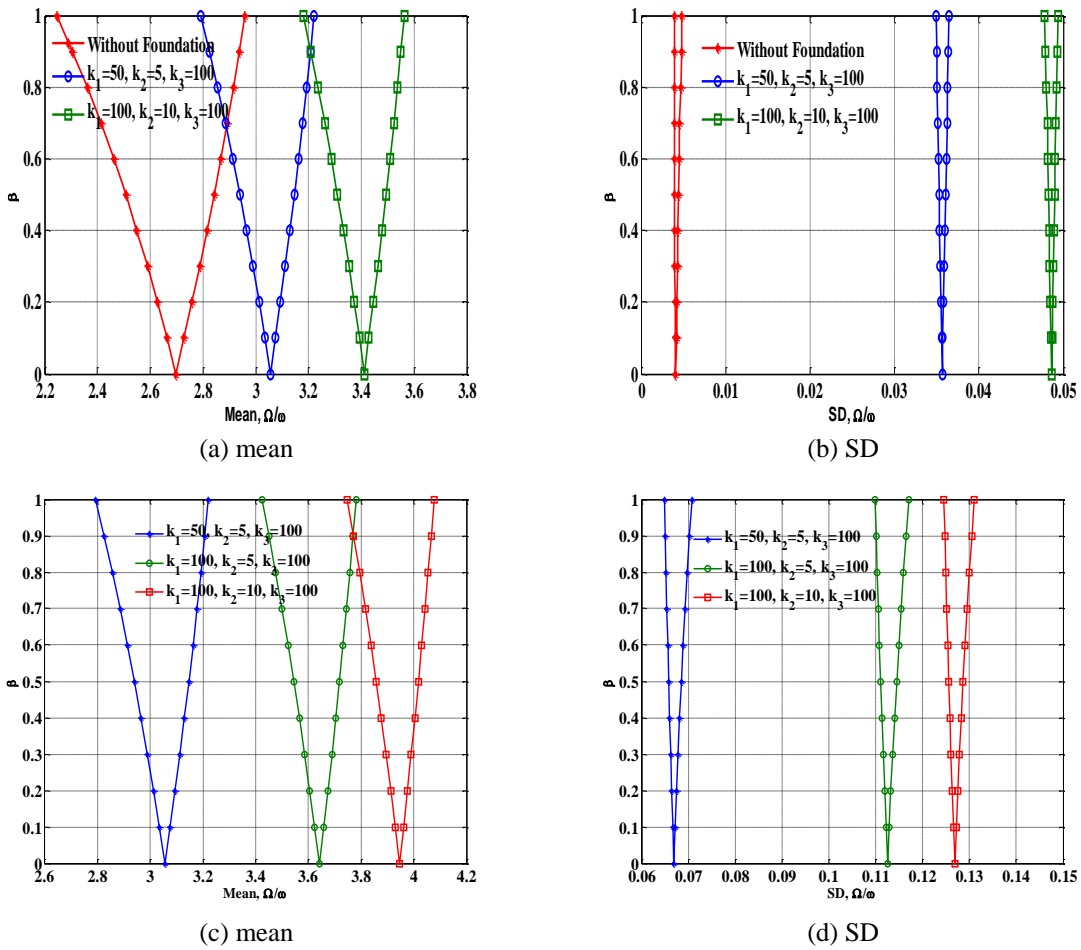


Fig. 11 Effect of thefoundation parameters on the dynamic instability of piezoelectric FGM beam

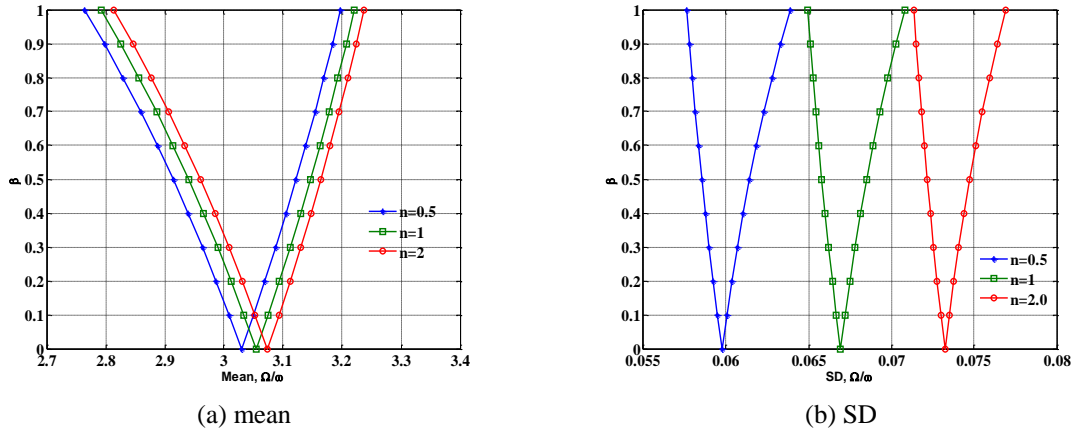


Fig. 12 Effect of the volume fraction exponents on the dynamic instability region of piezoelectric FGM beam

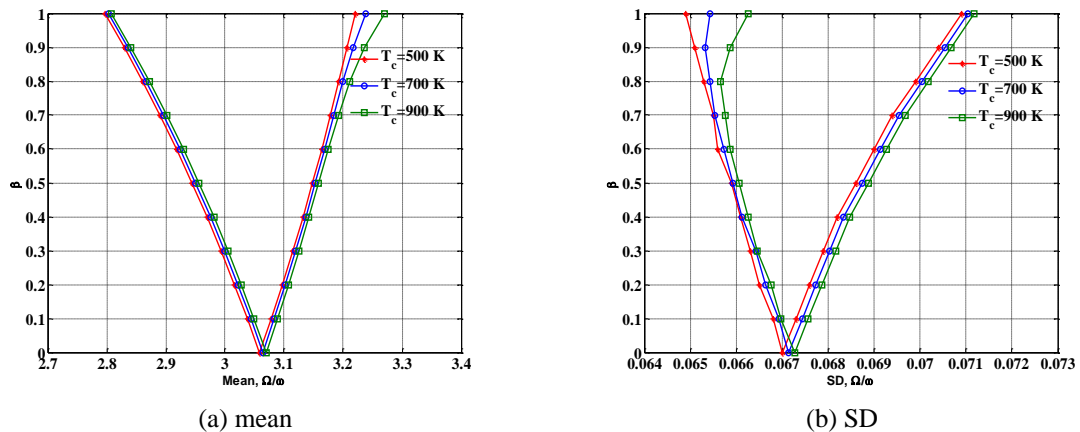


Fig. 13 Effect of the temperature variation on top surface on the dynamic instability region of FGM beam

frequency and width of the instability regions becomes narrow. Further, among the given different combination of foundation parameters, the effect of shear foundation on the dynamic instability is highest as compared to other foundation parameters. This is due to the fact that the foundation parameters increase the effective stiffness matrix that makes the beam more stable. The effect of the shear foundation parameter is most dominant to increase the stability and possibilities of resonance conditions.

Fig. 12 (a)-(b) examines the effect of volume fraction exponents ( $n=0, 1.0, \text{ and } 2$ ) on the mean and SD  $\{b_i (i=1, \dots, 10)=0.1\}$  of dynamic instability of FGM beams with  $a/h=20$  (foundation parameters?). With the increase of volume fraction exponents, the origin of mean dynamic instability shifts to higher frequency excitation and the instability region becomes wider and maximum when beam is composed of metal only. Although, SD of dynamic instability shifted to higher excitation frequency and the corresponding region becomes narrow.

Fig. 13 (a)-(b) shows the effect of temperature variation on top surface of beam ( $T_c=500$  K, 700

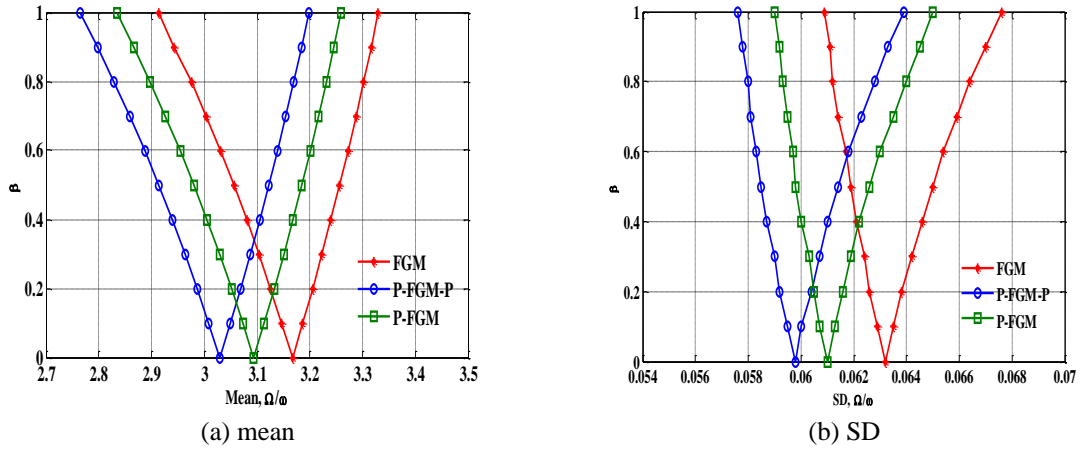


Fig. 14 Effect of the position of piezoelectric layer on the dynamic instability of piezoelectric FGM beams

K, and 900 K) with random change in system properties  $\{b_i (i=1, \dots, 10)=0.1\}$  on the mean and SD instability of piezoelectric FGMs beam resting with elastic foundation for  $n=1$  and  $a/h=20$ . With the increase of top surface temperature, the mean instability shifts to higher excitation and boundary region becomes wider. Although, origin of SD dynamic stability also shifted to higher excitation frequency and the instability region becomes narrow.

The effect of position of piezoelectric layers with random system properties  $\{b_i (i=1, \dots, 10)=0.1\}$  on the mean and SD of dynamic instability for simply supported FGM beams for volume fraction index  $n=0.5$  and  $a/h=20$  is shown in Fig. 14 (a)-(b). With the attachment of piezoelectric layers, the origin of mean dynamic stability shifted to lower excitation frequency and instability region becomes wider. Although, The origin of SD of dynamic instability also shifts to lower excitation frequency and instability region becomes narrow.

The appearance of beats the phenomenon displacement response of simply supported FGM beam supported by elastic foundation is shown in Fig. 15 (a)-(d). The beat phenomena

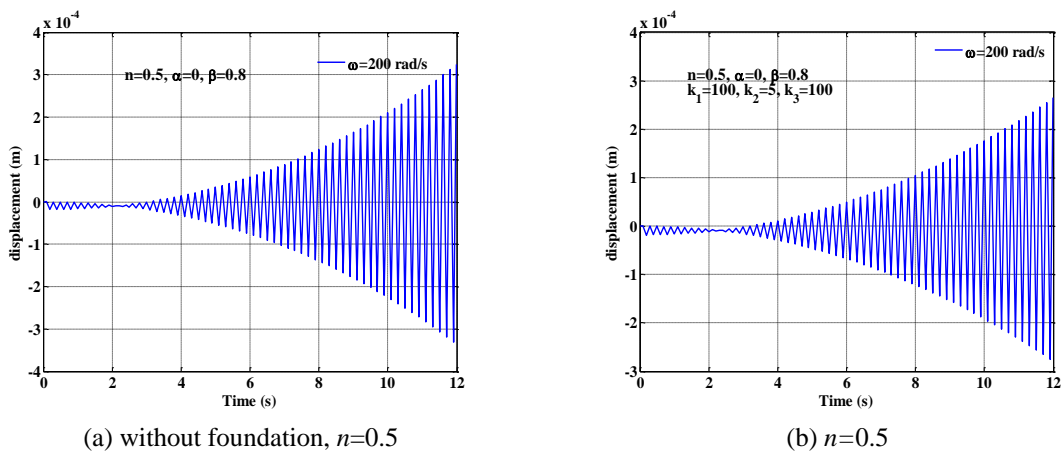
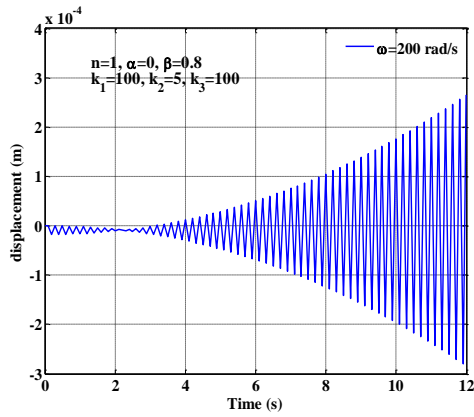
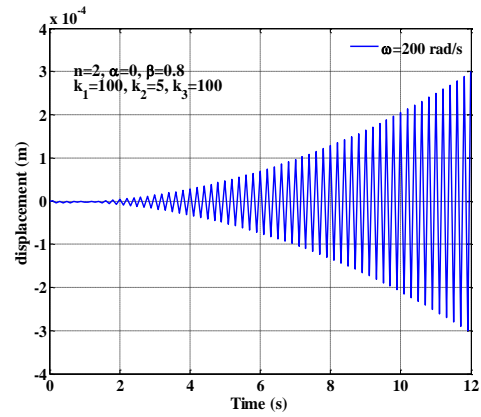


Fig. 15 Beat phenomena displacement response subjected to a periodic loading in unstable region for  $a/h=30$

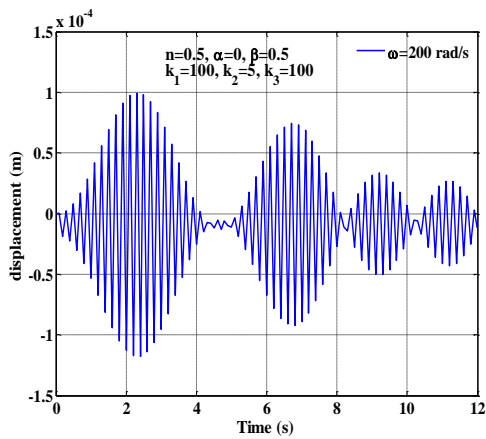


(c)  $n=1$

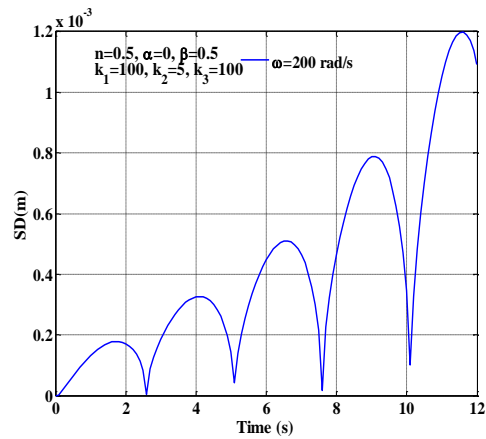


(d)  $n=2$

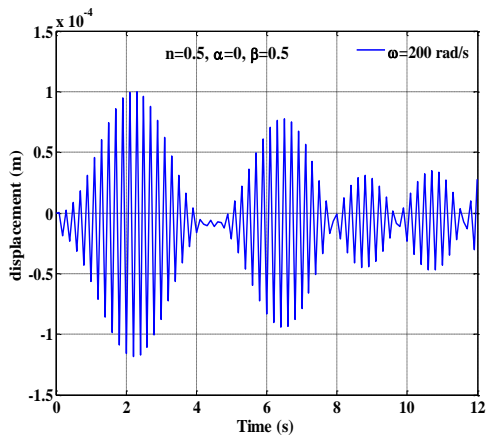
Fig. 15 Continued



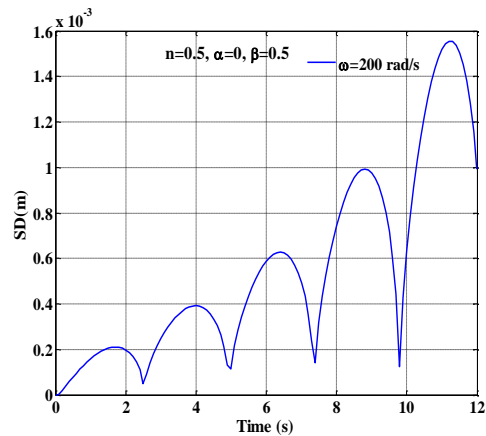
(a) mean dynamic displacement



(b) SD of dynamic displacement



(c) mean dynamic displacement



(d) SD of dynamic displacement

Fig. 16 Effect of foundation parameter on mean and SD of dynamic displacement for  $a/h=30$

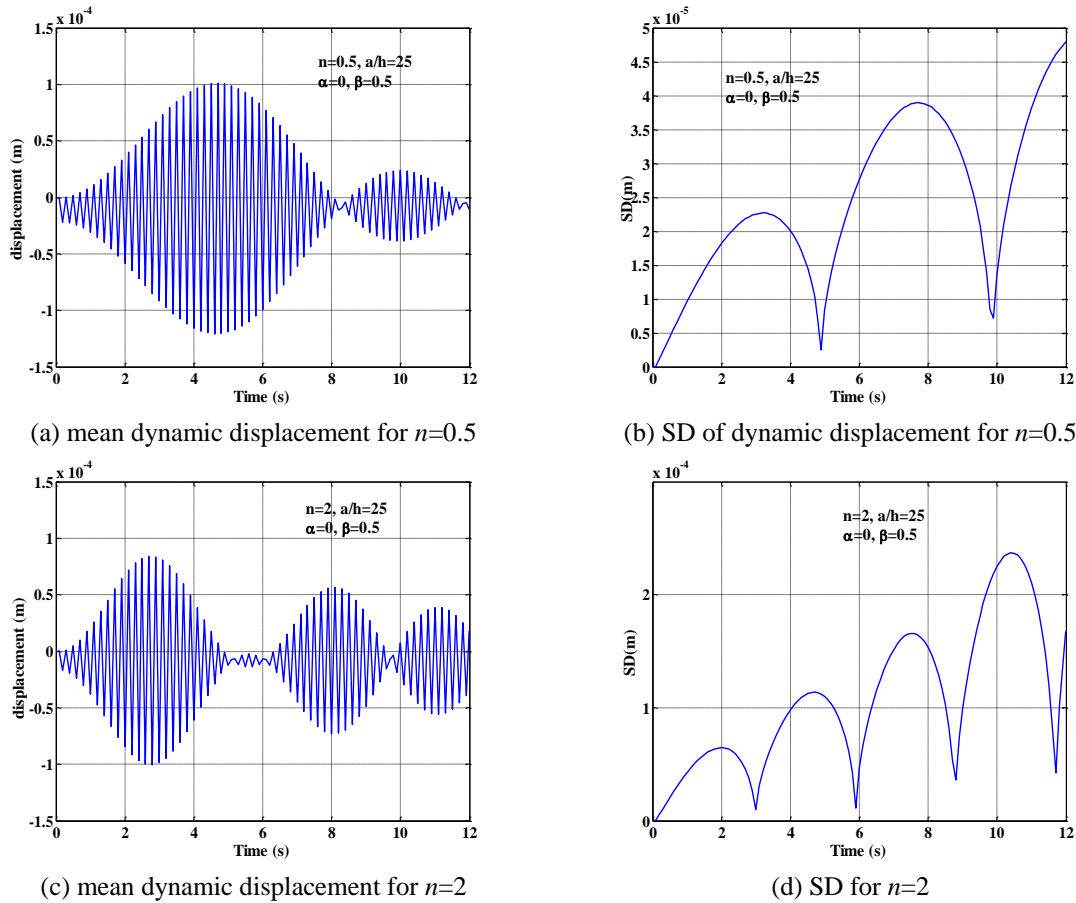


Fig. 17 Effect of volume fraction exponents on mean and SD of dynamic displacement

displacement response of a simply supported FGM beam supported with and without elastic foundation subjected to a periodic in-plane loading in the unstable region is examined. It is observed that the dynamic displacement of beam resting on elastic foundation is not much significant as compared to without foundation. The displacement response shows an increasing order due to the compressive periodic in-plane load under higher dynamic loading factor. The dynamic load parameters carrying the structure in unstable state is unreliable and hazardous and causes the structural failure. For this reason structure designer try to eliminate the instability of the structure with load control, nonlinearity and damping behavior of the structure.

Fig. 16 (a)-(d) shows the dynamic nonlinear displacement response of a simply supported piezoelectric FGM beam subjected to a periodic loading in unstable region for the beam supported with and without foundation for  $\beta=0.5$ ,  $\alpha=0.0$ ,  $n=1$ ,  $a/h=20$ .  $\omega=200$  rad/s. The beam supported by elastic foundation shows higher dynamic displacement as compared to beam without supported by elastic foundation. This is due to the fact that the foundation parameters increase the effective stiffness matrix of the beam which lower the bending resistance and beam becomes more stable.

Fig. 17 (a)-(d) shows the effect of volume fraction exponents on the nonlinear mean and SD of dynamic deflection with random change in  $\{b_i (i=1, \dots, 10)=0.1\}$  for  $\beta=0.5$ ,  $\alpha=0.5$  and  $W_{max}/h=0.5$ .

The effect of volume fraction exponent on mean dynamic displacement of beam is much significant as compared to higher volume fraction exponent. However, change of SD of dynamic deflection for a higher volume fraction exponent is higher than the lower volume fraction exponent. It is due to fact that at lower volume fraction exponent, the FGM beam contains a higher volume of ceramic portion.

## 7. Conclusions

In the FGM materials, as the amount of metal portion increases, the origin of instability regions becomes narrow and shifts to lower excitation frequency. Therefore, more amount of metal portions should be taken into consideration for stability of the structures.

With the presence of randomness at various levels, the origin of instability regions shifts to lower excitation frequency and the width of instability region increases. Hence, analysis of randomness of various randomness levels gives a more realistic picture of the parameters those are involved in safety in final design. Hence, the quantification of randomness is extremely important. Volume fraction exponents decrease the stability of the beam and increases the possibilities of resonance conditions.

As the amplitude ratio increase, the mean of dynamic instability shifts to higher excitation frequency and origin of dynamic instability regions becomes wider. Hence, the geometrical nonlinearity effect provides lower mean stability to the structures, however, vice versa for SD of dynamic stability.

Beam supported by elastic foundations provides higher mean dynamic stability and possibilities of higher resonance conditions. However, the SD of dynamic instability increases the possibilities of resonance conditions and lowers the dynamic stability. The effect of the shear foundation parameter is highly dominant as compared to linear and nonlinear Winkler foundation parameters. Hence, proper control of shear foundation is highly desirable for high safety of the elastically supported FGM beam.

The increments in temperature change decrease the mean stability of the beam and increases the possibilities of resonance conditions. However, SD of dynamic stability decreases the stability of beam and increases the possibilities of resonance conditions. Hence, it is concluded that temperature increments play an important role to decrease the stability and increases the possibilities of resonance conditions. The presence of piezoelectric layers decreases the mean and SD of stability of the beam and increases the possibility of resonance condition. The beat phenomenon of elastically supported FGM beam by changing the foundation parameter and volume fraction exponents is not so sensitive. However, the mean and SD of dynamic central deflection of FGM beam supported by elastic foundation are highly sensitive by increasing the foundation parameter and volume fraction exponents.

## References

- Abbas, B.A.H. and Thomas, J. (1978), "Dynamic stability of Timoshenko beams resting on an elastic foundation", *J. Sound Vib.*, **60**(1), 33-44.
- Ahuja, R. and Duffield, R.C. (1975), "Parametric instability of variable cross-section beams resting on an elastic foundation", *J. Sound Vib.*, **39**(2), 159-174.

- Baldinger, M., Belyaev, A.K. and Irschik, H. (2000), "Principal and second instability regions of shear-deformable polygonal plates", *Comput. Mech.*, **26**, 288-94.
- Bert, C.W. and Birman, V. (1987), "Dynamic instability of shear deformable antisymmetric angle-ply plates", *Int. J. Solid Struct.*, **23**(7), 1053-61.
- Bolotin, V.V. (1964), *The Dynamic Stability of Elastic Systems*, Holden-Day, Oakland, Calif.
- Chang, T.P. and Chang, H.C. (1994), "Stochastic dynamic finite element analysis of a non uniform beam", *Int. J. Solid Struct.*, **31**(5), 587-597.
- Chattopadhyay, A. and Radu, A.G. (2000), "Dynamic instability of composite laminates using a higher order theory", *Comput. Struct.*, **77**, 453-60.
- Chen, L.W. and Yang, J.Y. (1990), "Dynamic stability of laminated composite plates by the finite element method", *Comput. Struct.*, **36**, 845-51.
- Darabi, M., Darvizeh, M. and Darvizeh, A. (2007), "Non-linear analysis of dynamic stability for functionally graded cylindrical shells under periodic axial loading", *Compos. Struct.*, **83**(2), 201-11.
- Datta, P.K. and Chakraborty S. (1982), "Parametric instability of tapered beam by finite element method", *J. Mech. Eng.*, **24**(4), 205.
- Dey, S.S. (1979), "Finite element method for random response of structures due to stochastic excitation", *Comput. Meth. Appl. Mech. Eng.*, **20**(2), 173-194.
- Evan-Iwanowski, R.M. (1965), "The parametric response of structures", *Appl. Mech. Rev.*, **18**, 699-702.
- Fallah, A. and Aghdam, M.M. (2011), "Nonlinear free vibration and post buckling analysis of functionally graded beams on nonlinear elastic foundation", *Eur. J. Mech. A/Solid.*, **30**, 571-583.
- Fu, Y., Wang, J. and Mao, Y. (2012), "Nonlinear analysis of buckling, free vibration and dynamic stability for the piezoelectric functionally graded beams in thermal environment", *Appl. Math. Model.*, **36**(9), 4324-4340.
- Ganapathi, M., Boisse P. and Solaut D. (1999), "Non-linear dynamic stability analysis of composite laminates under periodic in-plane compressive loads", *Int. J. Numer. Meth. Eng.*, **46**, 943-956.
- Ganapathi, M., Varadan, T.K. and Balamurugan, V. (1994), "Dynamic instability of laminated composite curved panels using finite element method", *Compos. Struct.*, **53**, 335-42.
- Giuseppe, Q. (2011), "Finite element analysis with uncertain probabilities", *Comput. Meth. Appl. Mech. Eng.*, **200**(1-4), 114-129.
- Heyliger, P.R. and Reddy, J.N. (1988), "A higher order beam finite element for bending and vibration problems", *J. Sound Vib.*, **126**(2), 309-326.
- Hu, H.T. and Tzeng, W.L. (2000), "Buckling analysis of skew laminate plates subjected to uniaxial inplane loads", *Thin Wall Struct.*, **38**(1), 53-77.
- Ibrahim, R.A. (1987), "Structural dynamics with parameter uncertainties", *Appl. Mech. Rev.*, **40**(3), 309-328.
- Iwankiewicz, R. and Nielsen, S.R.K. (1999), *Advanced Method In Stochastic Dynamics of Nonlinear Systems*, Aalborg University Press.
- Jagtap, K.R., Lal, A. and Singh, B.N. (2011), "Stochastic nonlinear free vibration analysis of elastically supported functionally graded materials plate with system randomness in thermal environment", *Compos. Struct.*, **93**(12), 3185-3199.
- Jagtap, K.R., Lal, A. and Singh, B.N. (2013), "Thermomechanical elastic postbuckling of functionally graded materials plate with random system properties", *Int. J. Comp. Meth. Eng. Sci. Mech.*, **14**, 175-194.
- Kapania, R.K. and Park, S. (1996), "Nonlinear transient response and its sensitivity using finite elements in time", *Comput. Mech.*, **17**(5), 306-317.
- Kareem, A. and Sun W.J. (1990), "Dynamic response of structures with uncertain damping", *Eng. Struct.*, **12**(1), 2-8.
- Ke, L.L. and Wang, Y.S. (2011), "Size effect on dynamic stability of functionally graded microbeams based on a modified couple stress theory", *Compos. Struct.*, **93**(2), 342-350.
- Kiani, Y. and Eslami, M.R. (2010), "Thermal buckling analysis of functionally graded material beams", *Int. J. Mech. Mater. Des.*, **6**, 229-238.
- Kiani, Y. and Eslami, M.R. (2013), "Thermomechanical buckling of temperature dependent FGM beams", *Lat. Am. J. Solid Struct.*, **10**, 223-246.

- Kleiber, M. and Hien, T.D. (1992), *The Stochastic Finite Element Method*, John Wiley & Sons.
- Lal, A., Jagtap, K.R. and Singh, B.N. (2013), "Post buckling response of functionally graded materials plate subjected to mechanical and thermal loadings with random material properties", *Appl. Math. Model.*, **37**(7), 2900-2920.
- Lal, A., Kulkarni, N.M. and Singh, B.N. (2015), "Stochastic thermal post buckling response of elastically supported laminated piezoelectric composite plate using micromechanical approach", *Curv. Layer. Struct.*, **2**, 331-350.
- Lal, A., Saidane, N. and Singh, B.N. (2012a), "Stochastic hygrothermoelectromechanical loaded post buckling analysis of piezoelectric laminated cylindrical shell panels", *Smart Struct. Syst.*, **9**(6), 505-534.
- Lal, A., Singh, H. and Shegokar, N.L. (2012b), "FEM model for stochastic mechanical and thermal postbuckling response of functionally graded material plates applied to panels with circular and square holes having material randomness", *Int. J. Mech. Sci.*, **62**(1), 18-33.
- Liao, C.L. and Cheng, C.R. (1994), "Dynamic stability of stiffened laminated composite plates and shells subjected to in-plane pulsating forces", *Int. J. Numer. Meth. Eng.*, **37**, 4167-83.
- Liu, W.K., Belytschko, T. and Mani, A. (1986), "Probabilistic finite elements for nonlinear structural dynamics", *Comput. Meth. Appl. Mech. Eng.*, **56**(1), 61-81.
- Mohanty, S.C., Dash, R.R. and Rout, T. (2011), "Parametric instability of a functionally graded Timoshenko beam on Winkler's elastic foundation", *Nucl. Eng. Des.*, **241**(8), 2698- 2715.
- Moorthy, J. and Reddy, J.N. (1990), "Parametric Instability of laminated composite plates with transverse shear deformation", *Int. J. Solid. Struct.*, **26**, 801-811.
- Namachchivaya, N. and Lin, Y.K. (2003), *Nonlinear Stochastic Dynamics, Solid Mechanics and Its Applications*, Kluwar Academic publishers, Dordrecht.
- Nayfeh, A. (1993), *Introduction to Perturbation Techniques*, Wiley-Inter science.
- Ng, T.Y., Lam, K.Y., Liew, K.M. and Reddy, J.N. (2001), "Dynamic stability analysis of functionally graded cylindrical shells under periodic axial loading", *Int. J. Solid. Struct.*, **38**(8), 1295-1309.
- Nigam, N.C. and Narayanan, S. (1994), *Applications of Random Vibrations*, Narosa, New Delhi.
- Onkar, A.K. and Yadav, D. (2005), "Forced nonlinear vibration of laminated composite plates with random material properties", *Compos. Struct.*, **70**(3), 334-342.
- Patel, B.P., Singh, S. and Nath, Y. (2006), "Stability and nonlinear dynamic behaviour of cross-ply laminated heated cylindrical shells", *Lat. Am. J. Solid. Struct.*, **3**, 245-26.
- Pradyumna, S. and Bandyopadhyay, J.N. (2010), "Dynamic instability of functionally graded shells using higher-order theory", *J. Eng. Mech.*, **136**(5), 551-561.
- Raj, B.N., Iyengar, N.G.R. and Yadav, D. (1998), "Response of composite plates with random material properties using Monte Carlo Simulation", *Adv. Compos. Mater.*, **7**(3), 219-237.
- Ren, Y.J., Elishakoff, I. and Shinozuka, M. (1997), "Finite element method for stochastic beams based on variational principles", *J. Appl. Mech.*, **64**(3), 664-669.
- Rollot, O. and Elishakoff, I. (2003), "Large variation finite element method for beams with stochastic stiffness", *Chao. Solit. Fract.*, **17**(4), 749-779.
- Sahu, S.K. and Datta, P.K. (2007), "Research advances in the dynamic stability behavior of plates and shells: 1987-2005 Part I: conservative system", *Appl. Mech. Rev.*, **60**, 65-75.
- Shaker, A., Abdelrahman, W., Tawfik, M. and Sadek, E. (2008), "Stochastic finite element analysis of the free vibration of laminated composite plates", *Comput. Mech.*, **41**, 493-501.
- Shegokar, N.L. and Lal, A. (2013a), "Stochastic nonlinear bending response of piezoelectric functionally graded beam subjected to thermoelectromechanical loadings with random material properties", *Compos. Struct.*, **100**, 17-33.
- Shegokar, N.L. and Lal, A. (2013b), "Stochastic finite element nonlinear free vibration analysis of piezoelectric functionally graded beam subjected to thermo-piezoelectric loadings with material uncertainties", *Meccanica*, **49**, 1039-1068.
- Shegokar, N.L. and Lal, A. (2014), "Thermoelectromechanically induced stochastic post buckling response of piezoelectric functionally graded beam", *Int. J. Mech. Mater. Des.*, **10**, 329-349.
- Shinozuka, M. and Astill, C.J. (1972), "Random eigenvalue problems in structural analysis", *AIAA J.*, **10**(4),

- 456-462.
- Singha, M.K., Ramachandra, L.S. and Bandyopadhyay, J.N. (2001), "Stability and strength of composite skew plates under thermomechanical loads", *Am. Inst. Aeronaut. J.*, **39**(8), 1618-23.
- Srinivasan, R.S. and Chellapandi, P. (1986), "Dynamic stability of rectangular laminated composite plates", *Comput. Struct.*, **24**(2), 233-8.
- Stefanou, G. (2009), "The stochastic finite element method: Past, present and future, Engineering", *Comput. Meth. Appl. Mech. Eng.*, **198**(9), 1031-1051.
- Vanmarcke, E. and Grigoriu, M. (1983), "Stochastic finite element analysis of simple beams", *J. Eng. Mech.*, **109**(5), 1203-1214.
- Wang, S. and Dawe, D.J. (2002), "Dynamic instability of composite laminated rectangular plates and prismatic plate structures", *Comput. Meth. Appl. Mech. Eng.*, **191**, 1791-826.
- Wu, L., Wang, H.J. and Wang, D.B. (2007), "Dynamic stability analysis of FGM plates by the moving least squares differential quadrature method", *Compos. Struct.*, **77**(3), 383-394.
- Yang, J., Liew, K.M. and Kitipornchai, S. (2004), "Dynamic stability of laminated FGM plates based on higher-order shear deformation theory", *Comput. Mech.*, **33**(4), 305-315.
- Yang, J., Liew, K.M. and Kitipornchai, S. (2005), "Stochastic analysis of compositionally graded plates with system randomness under static loading", *Int. J. Mech. Sci.*, **47**(10), 1519-1541.
- Young, T.H. and Chen, F.Y. (1994), "Stability of skew plates subjected to aerodynamic and in-plane forces", *J. Sound Vib.*, **171**(5), 603-15.
- Zhao, L. and Chen, Q. (1998), "A dynamic stochastic finite element method based on dynamic constraint mode", *Comput. Meth. Appl. Mech. Eng.*, **161**(3-4), 245-25.
- Zhu, J., Chen, C., Shen, Y. and Wang, S. (2005), "Dynamic stability of functionally graded piezoelectric circular cylindrical shells", *Mater. Lett.*, **59**(4), 477-85.

## Appendix

$$[T] = \begin{bmatrix} 1 & z & z^3 & 0 & 0 \\ 0 & 0 & 0 & 1 & z^2 \end{bmatrix}, [L] = \begin{bmatrix} \frac{\partial}{\partial x} & 0 & 0 & 0 & \frac{\partial}{\partial x} & 0 & 0 & 0 \\ 0 & 0 & 0 & \frac{\partial}{\partial x} & 0 & 0 & 0 & \frac{\partial}{\partial x} \\ 0 & -C_4 \frac{\partial}{\partial x} & -C_2 \frac{\partial}{\partial x} & 0 & 0 & -C_4 \frac{\partial}{\partial x} & -C_2 \frac{\partial}{\partial x} & 0 \\ 0 & C_1 \frac{\partial}{\partial x} & 0 & C_1 & 0 & C_1 \frac{\partial}{\partial x} & 0 & C_1 \\ 0 & 0 & -3C_4 & -3C_4 & 0 & 0 & -3C_4 & -3C_4 \end{bmatrix} \quad (\text{A-1})$$

$$D = \int_{-h/2}^{h/2} [T]^T [\bar{Q}] [T] dz = \begin{bmatrix} A_{11} & B_{11} & E_{11} & 0 & 0 \\ B_{11} & D_{11} & F_{11} & 0 & 0 \\ E_{11} & F_{11} & H_{11} & 0 & 0 \\ 0 & 0 & 0 & A_{55} & D_{55} \\ 0 & 0 & 0 & D_{55} & F_{55} \end{bmatrix} \quad (\text{A-2a})$$

$$(A_{11}, B_{11}, D_{11}, E_{11}, F_{11}, H_{11}) = \int_{-h/2}^{h/2} Q_{11}(1, z, z^2, z^3, z^4, z^6) dz \quad \text{and} \quad (A_{55}, D_{55}, F_{55}) = \int_{-h/2}^{h/2} Q_{55}(1, z^2, z^4) dz$$

$$[D_1] = \int_{-h/2}^{h/2} [T]^T [e] [T] dz = \begin{bmatrix} [0] & [0] & [0] & [M_{11}] & [N_{11}] \\ [0] & [0] & [0] & [N_{11}] & [P_{11}] \\ [0] & [0] & [0] & [P_{11}] & [R_{11}] \\ [M_{22}] & [N_{22}] & [P_{22}] & [0] & [0] \\ [N_{22}] & [P_{22}] & [R_{22}] & [0] & [0] \end{bmatrix} \quad (\text{A-2b})$$

$$(M_{11}, N_{11}, P_{11}, R_{11}) = \int_{-h/2}^{h/2} e_{15}(1, z, z^2, z^3) dz \quad (M_{22}, N_{22}, P_{22}, R_{22}) = \int_{-h/2}^{h/2} e_{31}(1, z, z^2, z^3) dz$$

$$[D_2] = \int_{-h_p/2}^{h_p/2} [T_\phi] [\xi] [T_\phi] dz = \begin{bmatrix} [S_{11}] & [T_{11}] & [U_{11}] & [0] & [0] \\ [T_{11}] & [U_{11}] & [V_{11}] & [0] & [0] \\ [U_{11}] & [V_{11}] & [W_{11}] & [0] & [0] \\ [0] & [0] & [0] & [S_{22}] & [T_{22}] \\ [0] & [0] & [0] & [T_{22}] & [U_{22}] \end{bmatrix} \quad (\text{A-2c})$$

$$(S_{11}, T_{11}, U_{11}, V_{11}, W_{11}) = \int_{-h/2}^{h/2} k_{11}(1, z, z^2, z^3, z^4) dz \quad (S_{22}, T_{22}, U_{22}) = \int_{-h/2}^{h/2} k_{33}(1, z, z^2) dz,$$

$$D_3 = \begin{bmatrix} A_{11} & B_{11} & E_{11} & 0 & 0 \\ 0 & 0 & 0 & A_{55} & D_{55} \end{bmatrix}^T, D_4 = [D_3]^T, D_5 = \begin{bmatrix} A_{11} & 0 \\ 0 & A_{55} \end{bmatrix}, D_6 = \begin{bmatrix} 0 & 0 & 0 & M_{11} & N_{11} \\ M_{22} & N_{22} & P_{22} & 0 & 0 \end{bmatrix}, D_7 = [D_6]^T \quad (\text{A-3})$$